Quantum Dot Laser

Johann Peter Reithmaier

Technische Physik

Institute of Nanostructure Technologies & Analytics (INA)

University of Kassel

Tutorial for WWW.BRIGHTER.EU

Lund, 29.6.2007

INA

WWW • BRIGHTER • EU

Outline

- Introduction and Some Basic Theory
  - density of states, gain function
  - dependence on dimensions

- Fabrication Technology
  - molecular beam epitaxy and Stranski-Krastanov growth mode
  - influence on geometry parameters

- Optical properties of real dots systems
  - single dot emission, higher order transitions
  - inhomogeneous linewidth, wetting layer

- Application examples of QD lasers
  - high power lasers (980 / 920 nm)
  - ultra-broadband lasers (1.55 µm)
  - ultra-fast broadband SOAs (1.55 µm)

Quantum Dot Laser

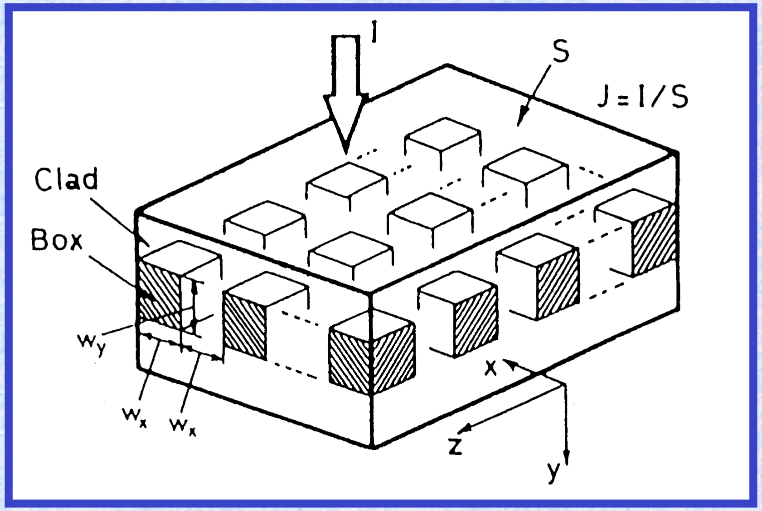

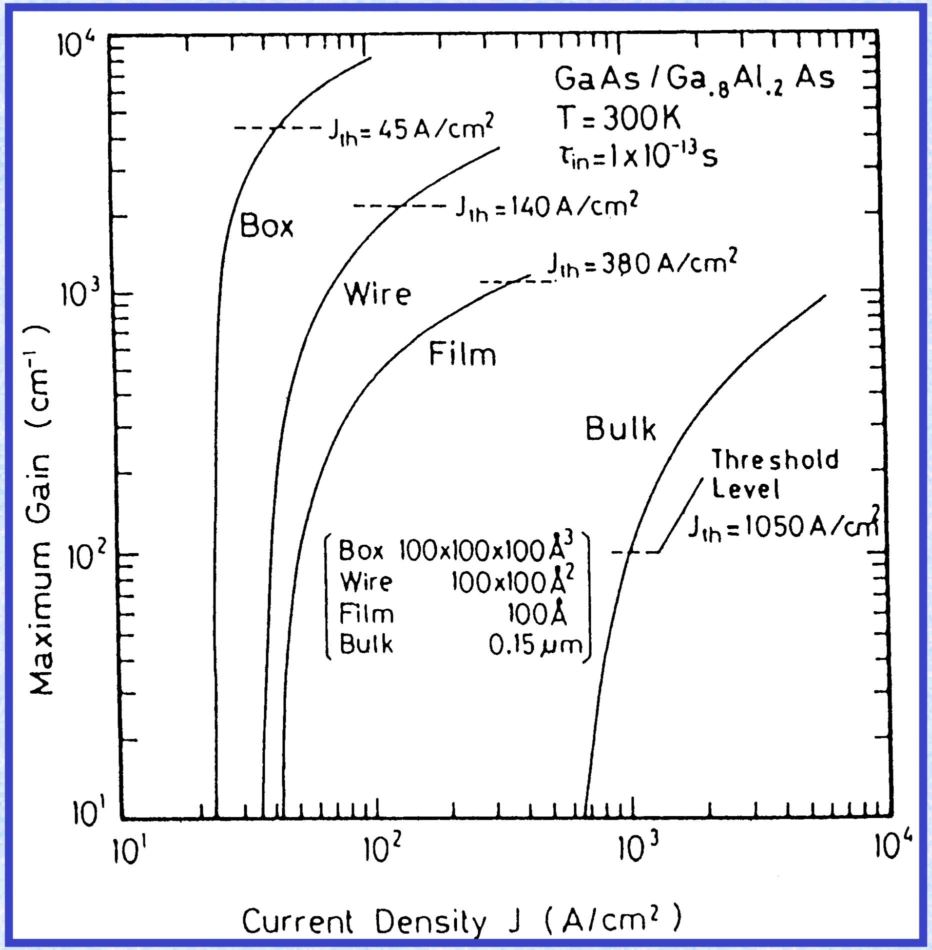

Due to higher density of states of quasi-zero dimensional systems a higher material and differential gain is expected in comparison to quantum well or bulk material

Also the transition matrix element has a higher value due to the improved overlapp of electron/hole wave functions.

M. Asada et al., IEEE JQE 22, 1915 (1986)

Time Evolution of Threshold Current Density

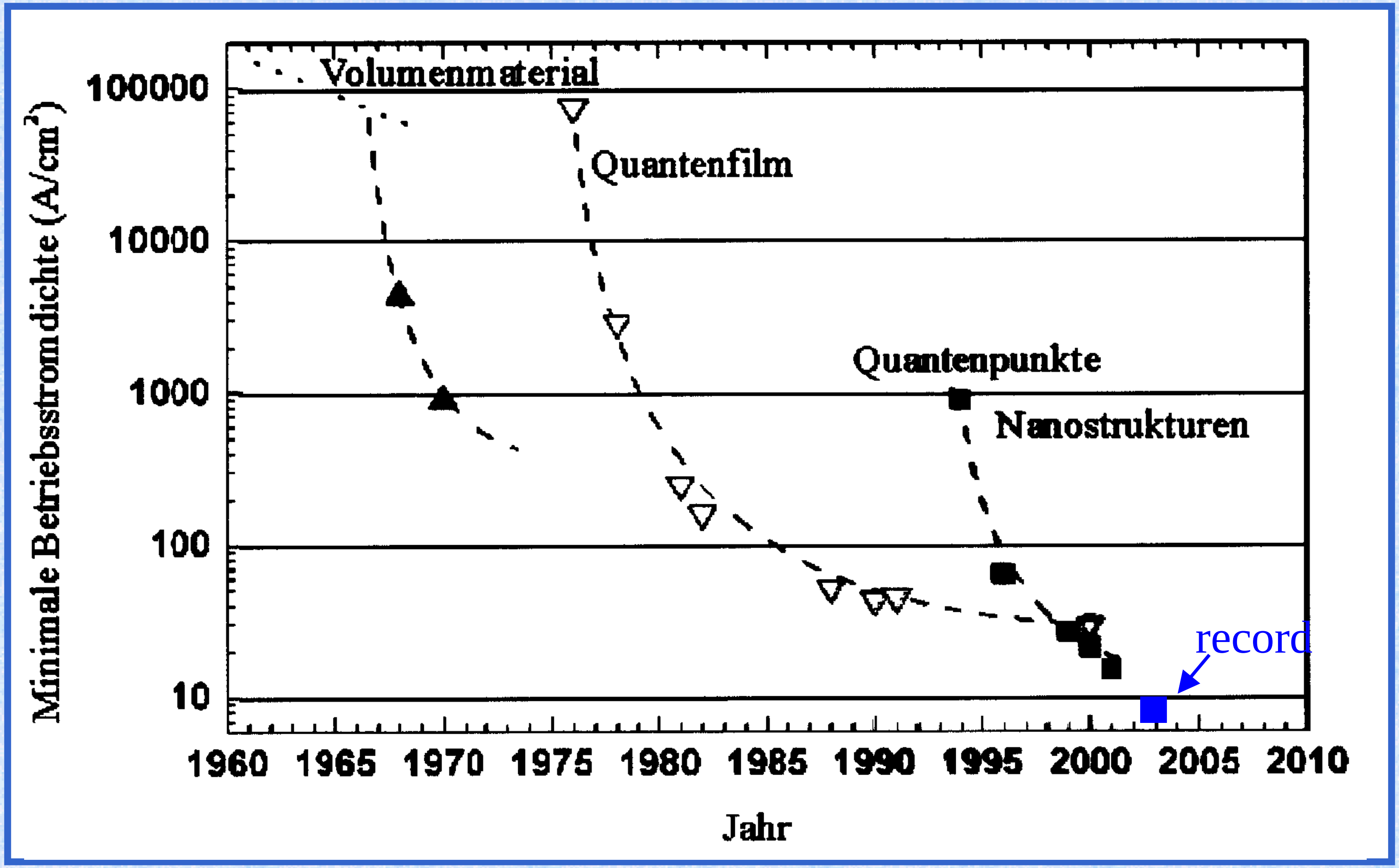

Optical Material Gain

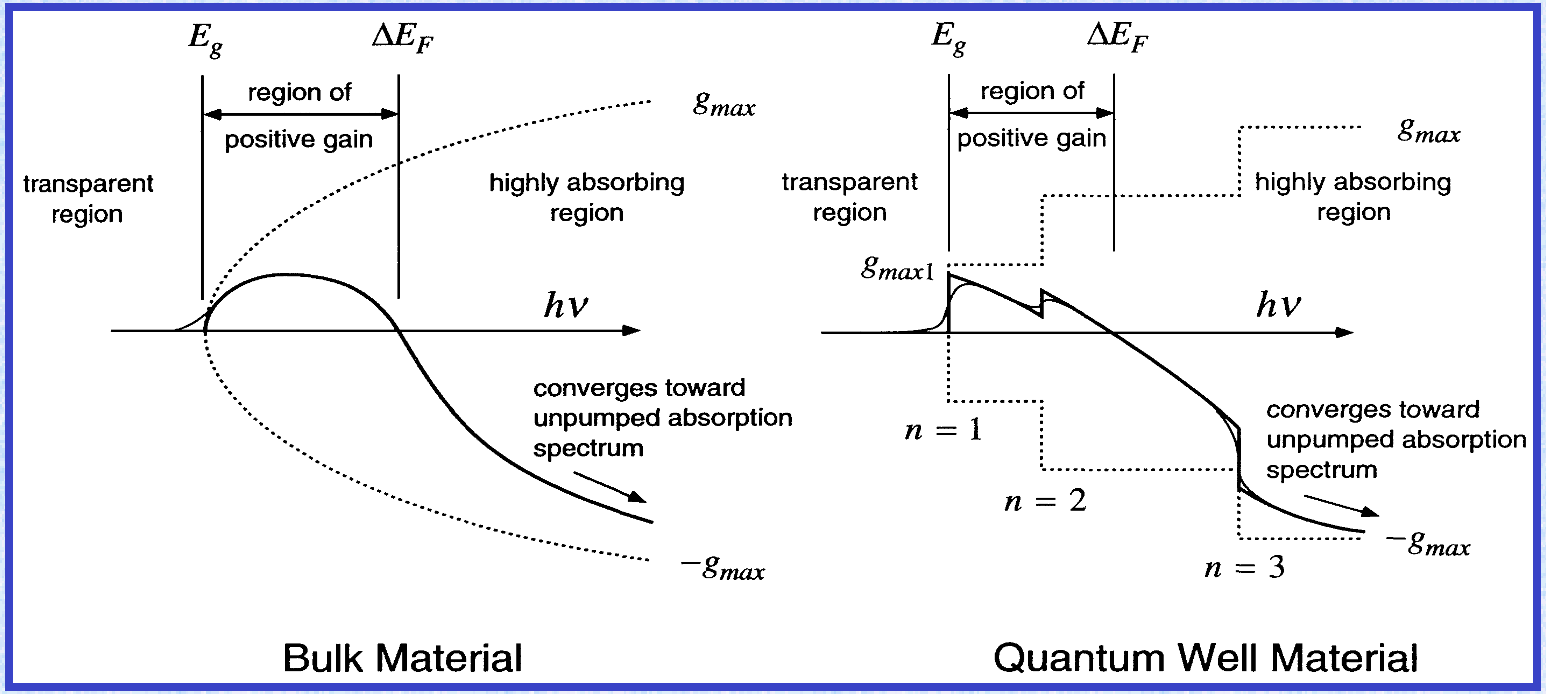

The gain can be changed by current injection between max. absorption (= $-g_{max}$) and max. gain (= g_{max}).

Spectral gain function

$$g(E_{21}) = \frac{\pi q^2 \hbar}{n \varepsilon_0 c m_0^2} \frac{1}{\hbar \omega_{21}} \left| M_T(E_{21}) \right|^2 \rho_r(E_{21})(f_2 - f_1) = g_{max}(E_{21}) \cdot (f_2 - f_1)$$

$\rho_r(E_{21})$ reduced density of state function

$M_T(E_{21})$ transition matrix element

L.A. Coldren, S.W. Corzine, "Diode Lasers and Photonic Integrated Circuits", Wiley, 1995.

Density of State Function for 2D Case

Number of states within circle of radius p:

$$N(p) = 2 \times \frac{\pi p^2}{(h/L)^2}$$

→ Density of state function in momentum space:

$$D(p) = \frac{dN}{dp} = \frac{4\pi p A}{h^2}$$

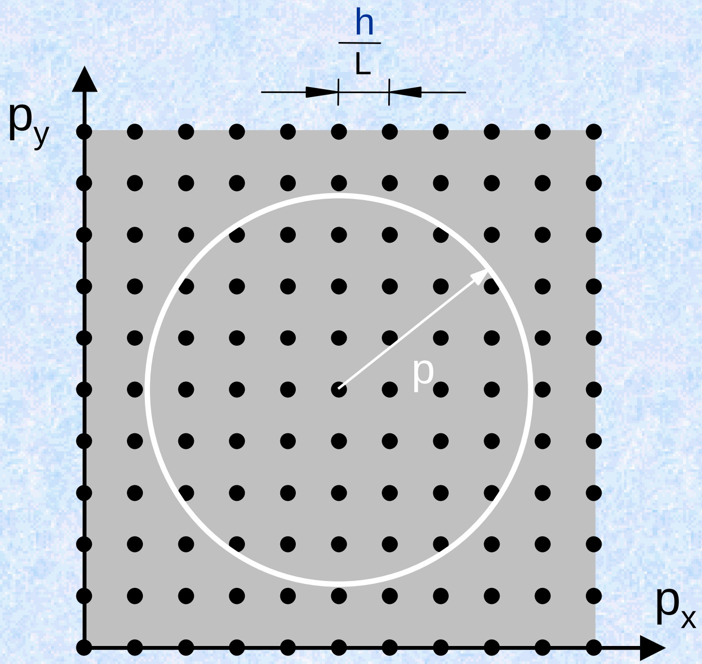

Density of state function as function of energy:

$$D(E) = \sum_{i=1}^{n} \frac{m^* L^2}{\pi \hbar^2} \Theta(E - E_i)$$

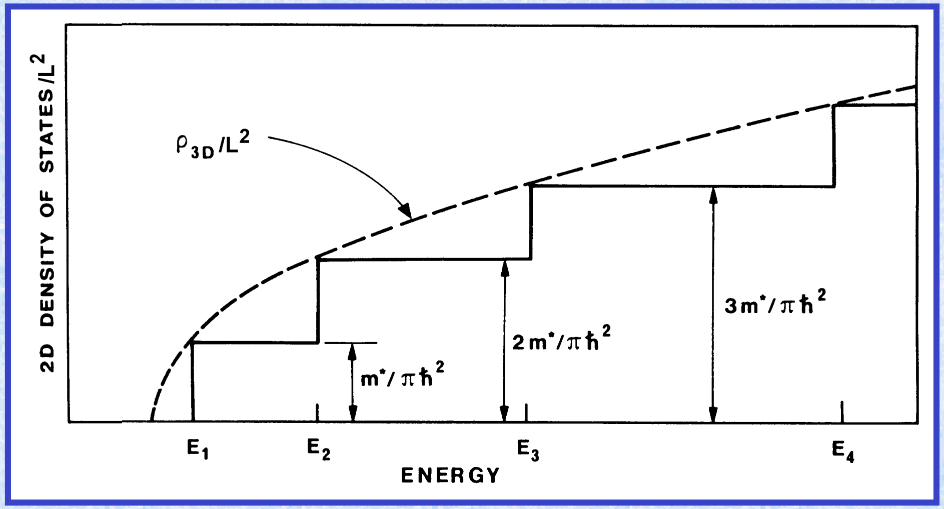

Density of State Functions in 1D and 0D

$$D(E) = \sum_{i=1}^{n} \sqrt{\frac{2m^* L^2}{\hbar^2}} \frac{1}{\pi \cdot \sqrt{E - E_i}} \Theta(E - E_i)$$

with Heaviside function Θ(E),
L as length of structure and
m* as effective mass of particle

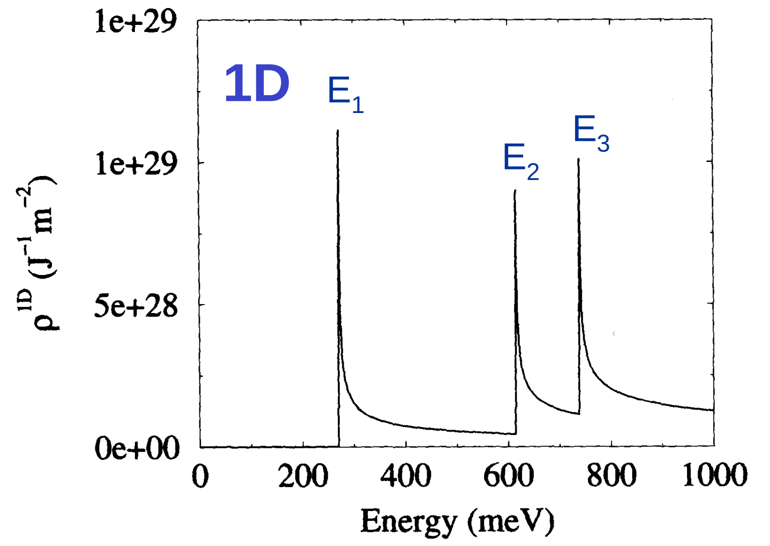

$$D(E) = \sum_{i=1}^{n} \alpha_i \cdot \delta(E - E_i)$$

with α_i as degeneracy
(= 2 for s orbitals)

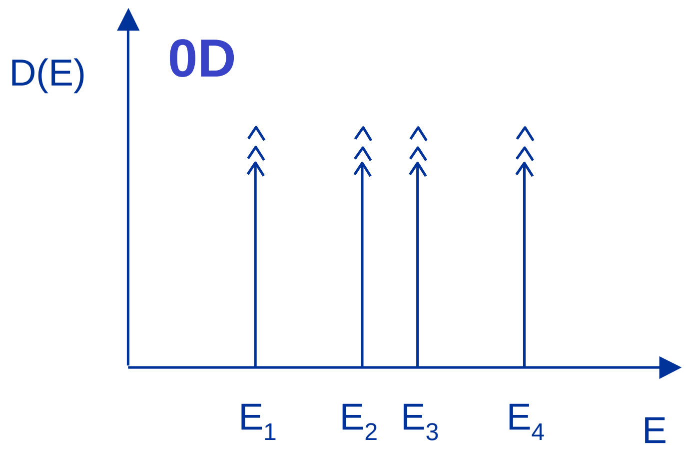

Density of State Dependence on Dimensionality

dimension	density of state D(p)	density of state D(E)
3D	$\frac{8\pi V}{h^3}\cdot(p)^2$	$\frac{V}{2\pi^2}\left(\frac{2m^*}{\hbar^2}\right)^{3/2}\cdot(E)^{\frac{1}{2}}$
2D	$\frac{4\pi A}{h^2}\cdot(p)^1$	$\frac{A}{2\pi}\left(\frac{2m^*}{\hbar^2}\right)^{1}\cdot(E)^{0}$
1D	$\frac{2L}{h}\cdot(p)^0$	$\frac{L}{\pi}\left(\frac{2m^*}{\hbar^2}\right)^{\frac{1}{2}}\cdot(E)^{-\frac{1}{2}}$
0D	$\delta(p-p_i)$	$\delta(E-E_i)$

Spectral Gain Function of QD Material

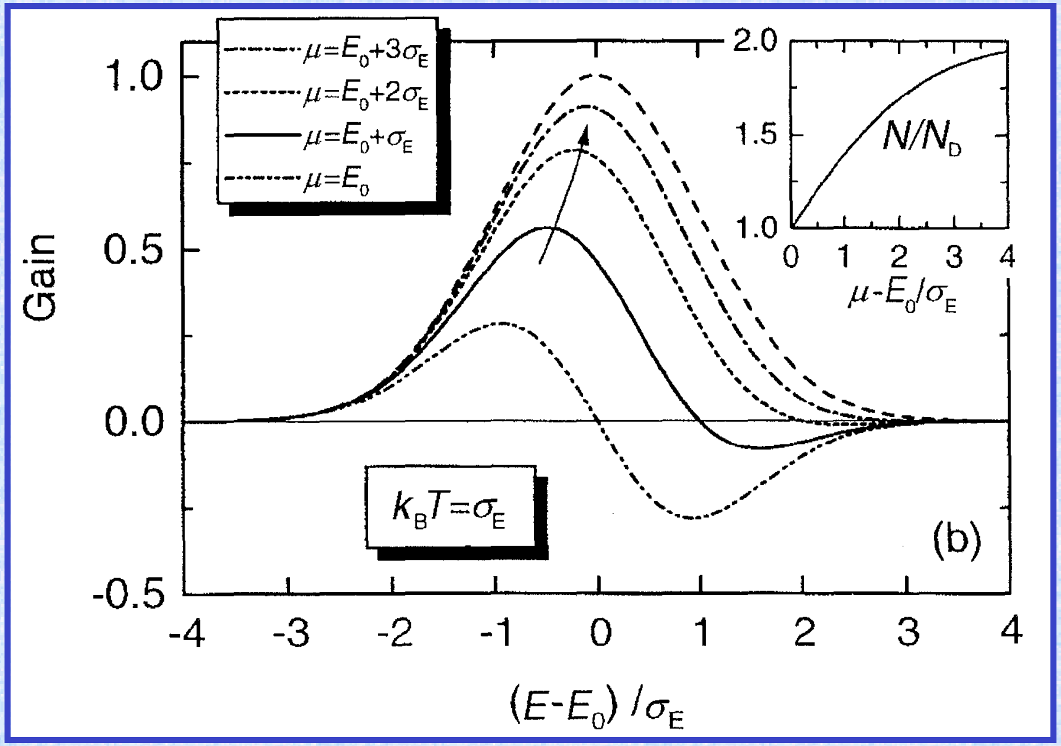

Spectral gain for inhomogenously broadened dot ensemble with one confined state

μ = chemical potential

σ_E = inhomogeneous linewidth

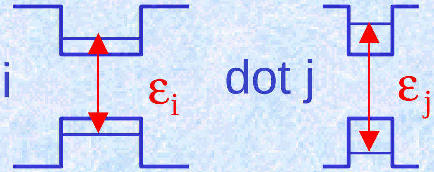

$$g(\hbar\omega)=\frac{\pi q^2\hbar}{n\varepsilon_0 c m_0^2}\frac{1}{\hbar\omega}\int\left|M_T(\hbar\omega)\right|^2\frac{2}{V_0}P(\varepsilon,\sigma_E)[f_c(\varepsilon,E_{Fc})-f_v(\varepsilon,E_{Fv})]\frac{\Gamma_{in}/\pi}{(\hbar\omega-\varepsilon)^2+\Gamma_{in}^2}d\varepsilon$$

with inhomogeneous ensemble linewidth:

$$P(\varepsilon,\sigma_E)=\frac{1}{\sigma_E\sqrt{2\pi}}\exp\left[-\frac{(\varepsilon-E_g-E_0)}{2\sigma_E^2}\right]$$

Lorentzian function of homogeneous linewidth

Gain Engineering with QD Properties

$$g_{mat}(E) \propto D(E) \times f(E,\mu)$$

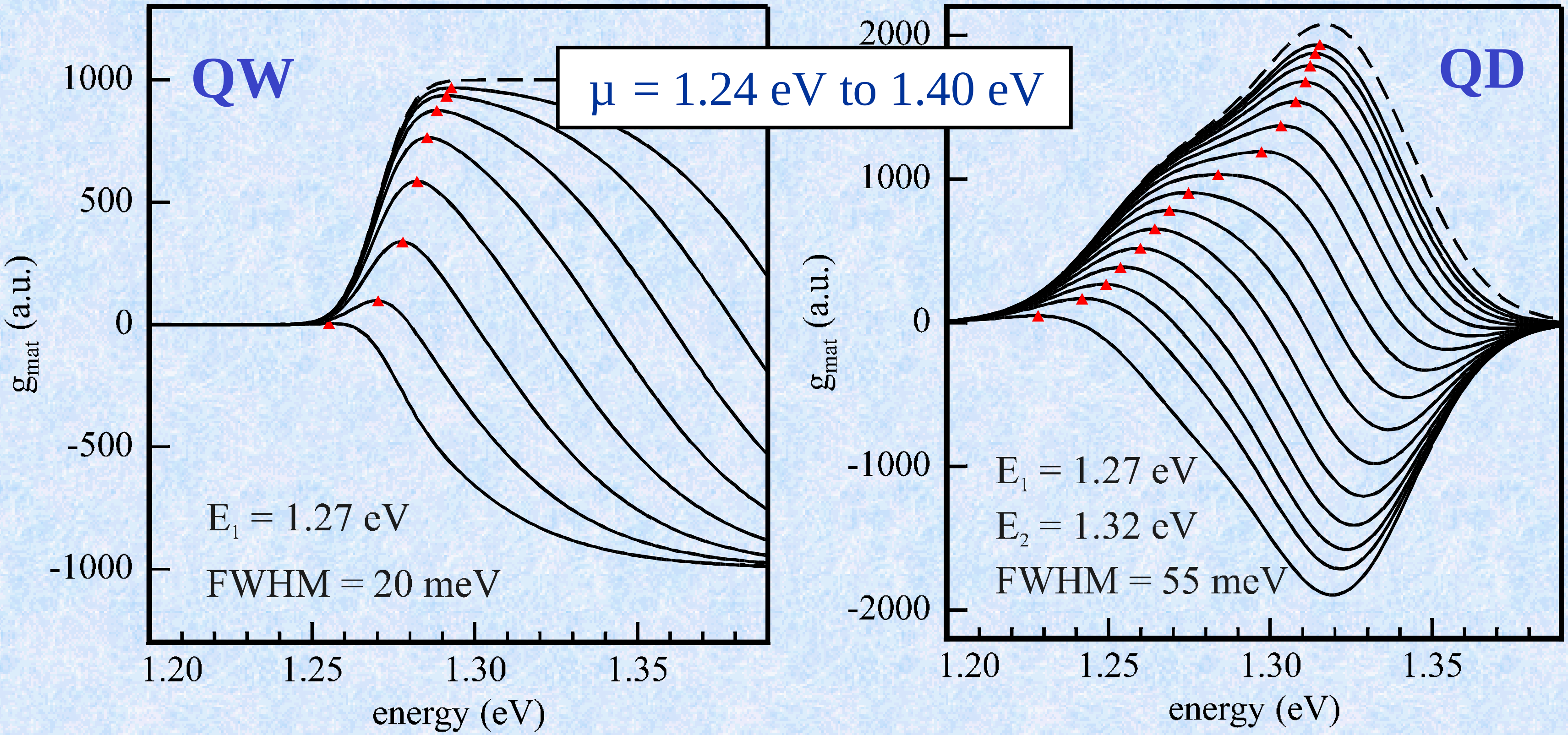

- Reduced blue shift due to high total gain
- After saturation of first transition large blue shift

F. Klopf et al., Photonics West, 2002

Comparison with Experimental Data

Gain profile evaluated by high power excitation PL experiment

→ Spectral gain function

Control of mirror losses by variation of cavity length

→ Variation of emission wavelength

$$g_{th} = \alpha_i + \frac{1}{L}\ln\left(\frac{1}{\sqrt{R_1 R_2}}\right)$$

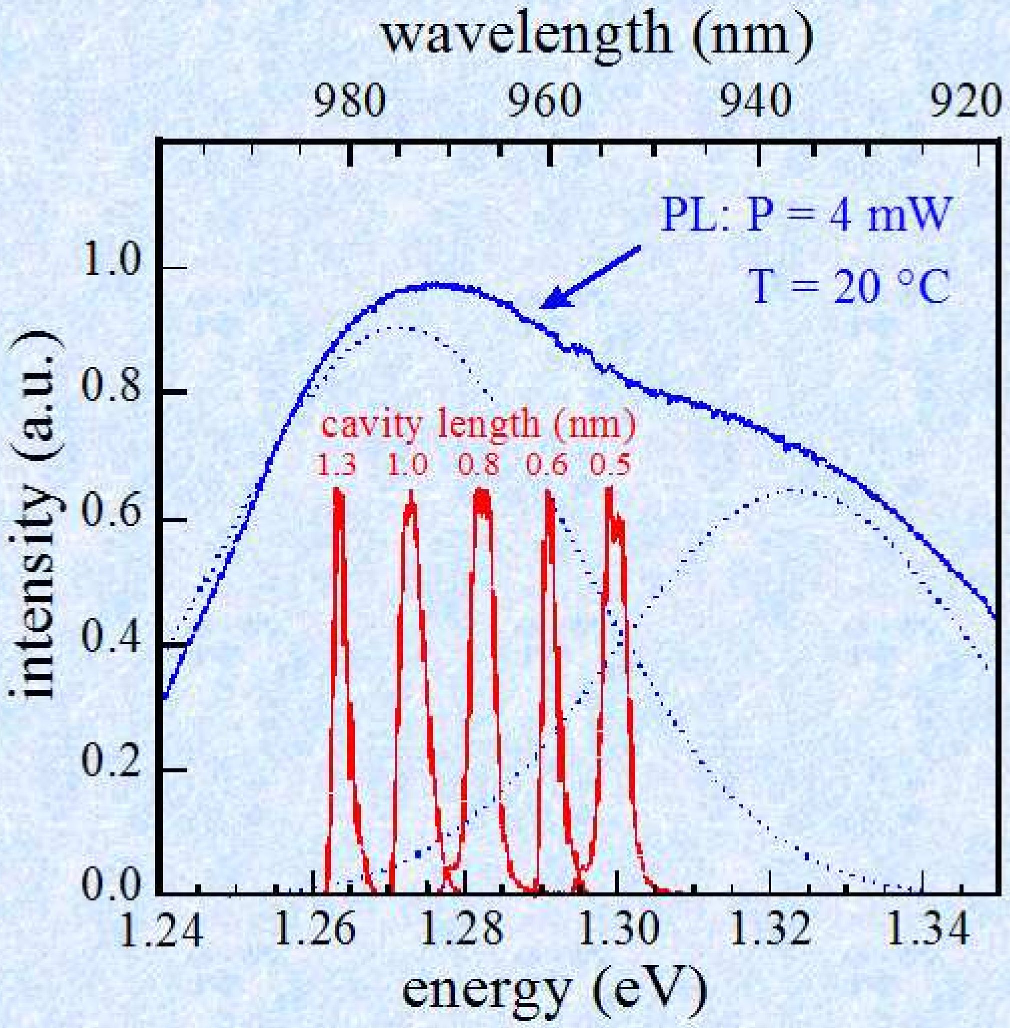

F. Klopf et al., Photonics West, 2002

Temperature Stability

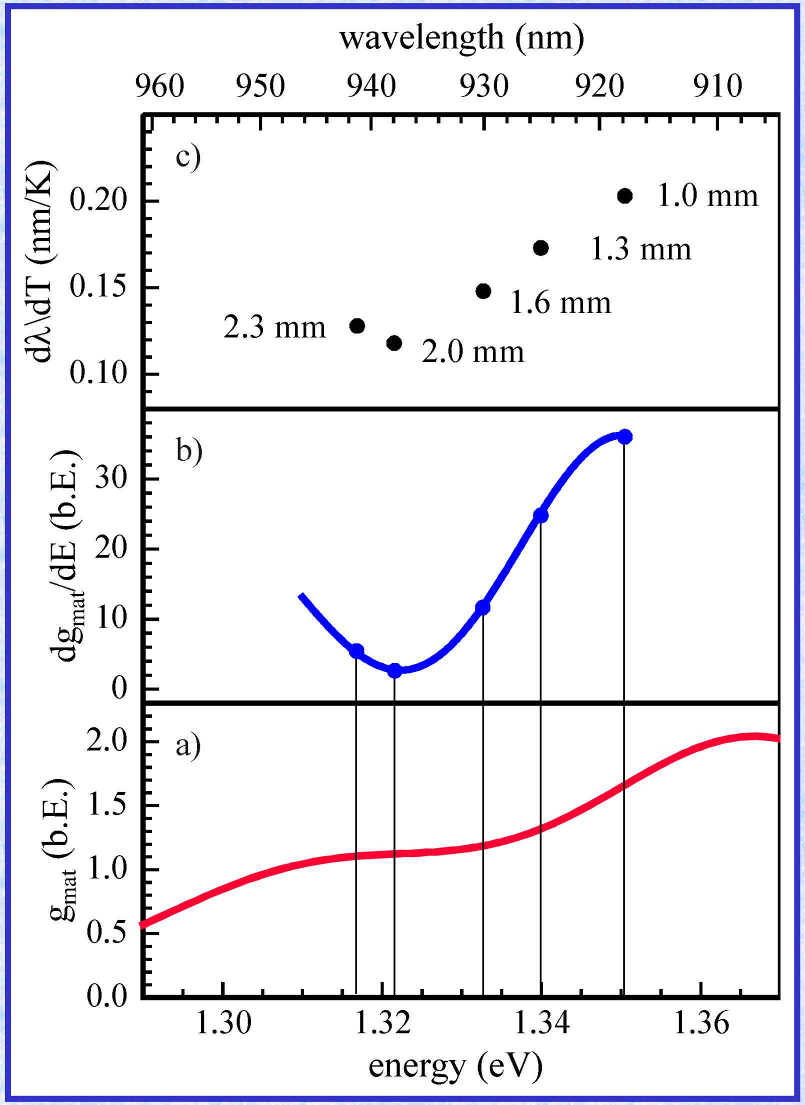

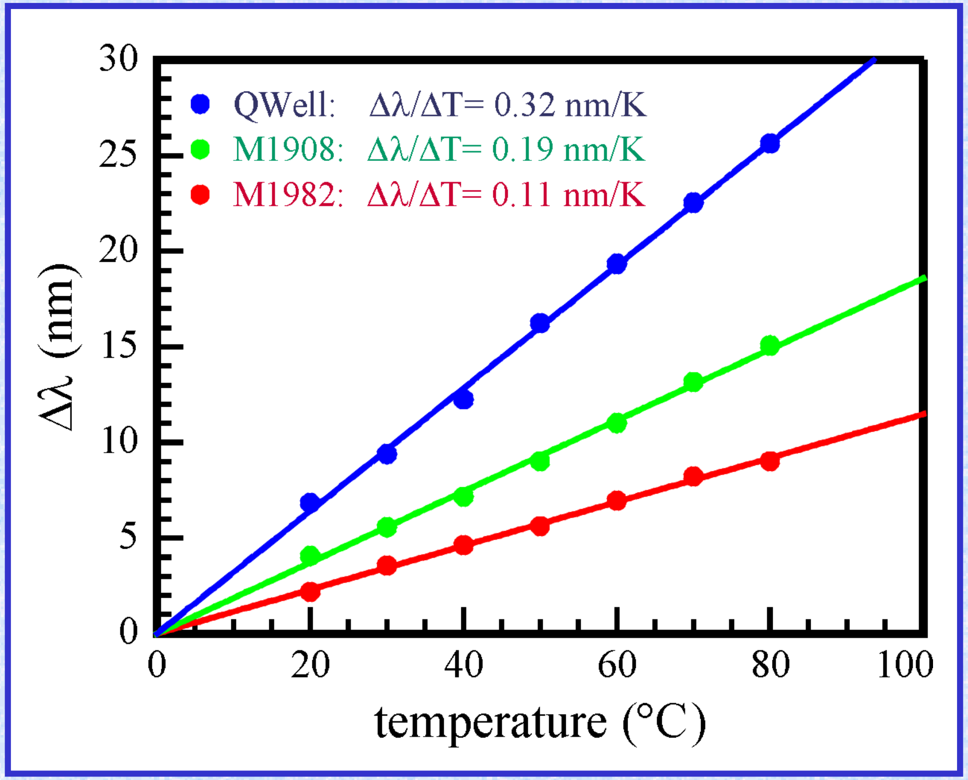

- Flat gain profile
- Very low temperature dependence of emission wavelength of 0.11 nm/K (best value for BA lasers: 0.09 nm/K)

Basic effect described in F. Klopf et al., APL 81, 217 (2002)

Specific Properties of QD Gain Material

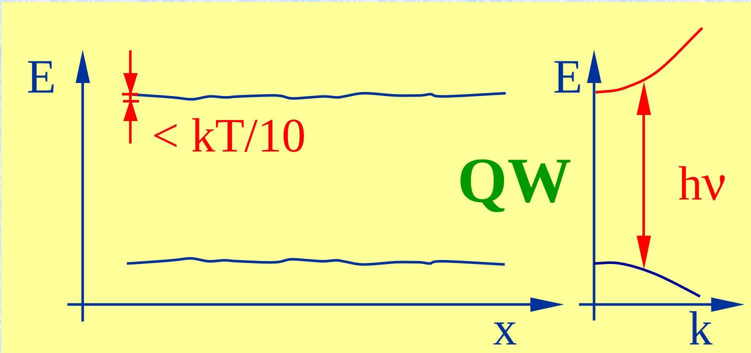

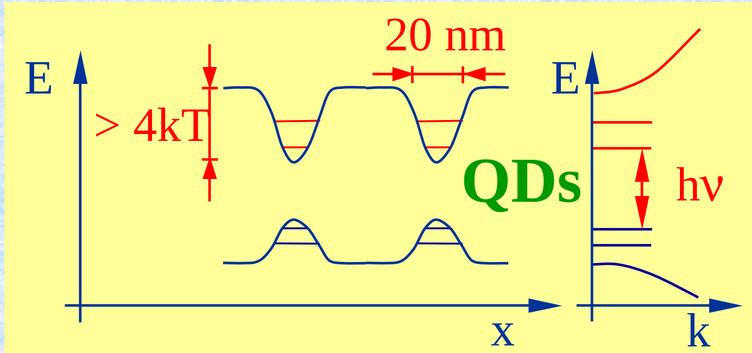

Discrete energy levels: → high density of states, no temperature dependence

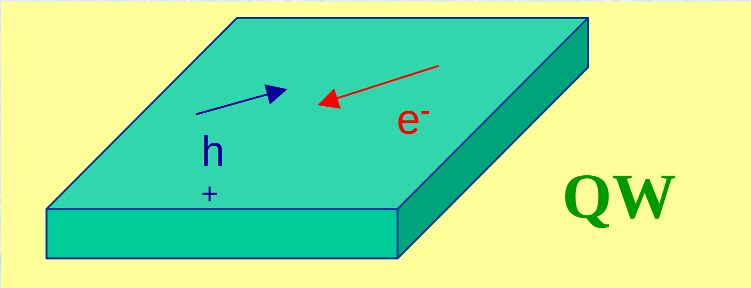

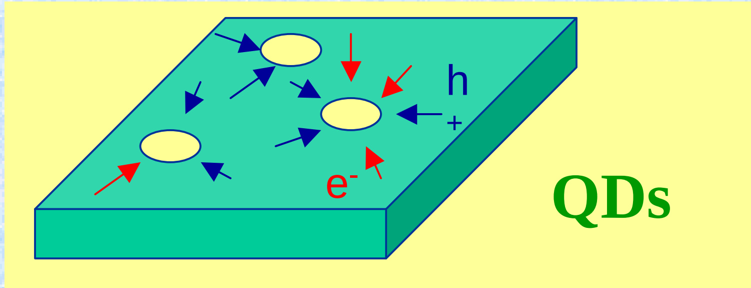

reduced diffusion: → no diffusion to surfaces

reduced active volume: → low absorption, low inversion densities

refractive index decoupled
from carrier density
+ symmetric gain function: → low chirp

$$\alpha = -\frac{4\pi}{\lambda}\frac{dn/dN}{dg/dN}$$

- Introduction and Some Basic Theory
  - density of states, gain function
  - dependence on dimensions

- Fabrication Technology
  - molecular beam epitaxy and Stranski-Krastanov growth mode
  - influence on geometry parameters

- Optical properties of real dots
  - single dot emission, higher order transitions
  - inhomogeneous linewidth, wetting layer

- Application examples of QD lasers
  - high power lasers (980 / 920 nm)
  - ultra-broad band lasers (1.55 µm)
  - ultra-fast broadband SOAs (1.55 µm)

Basic Phenomena During Epitaxial Growth

Example: Molekular Beam Epitaxy

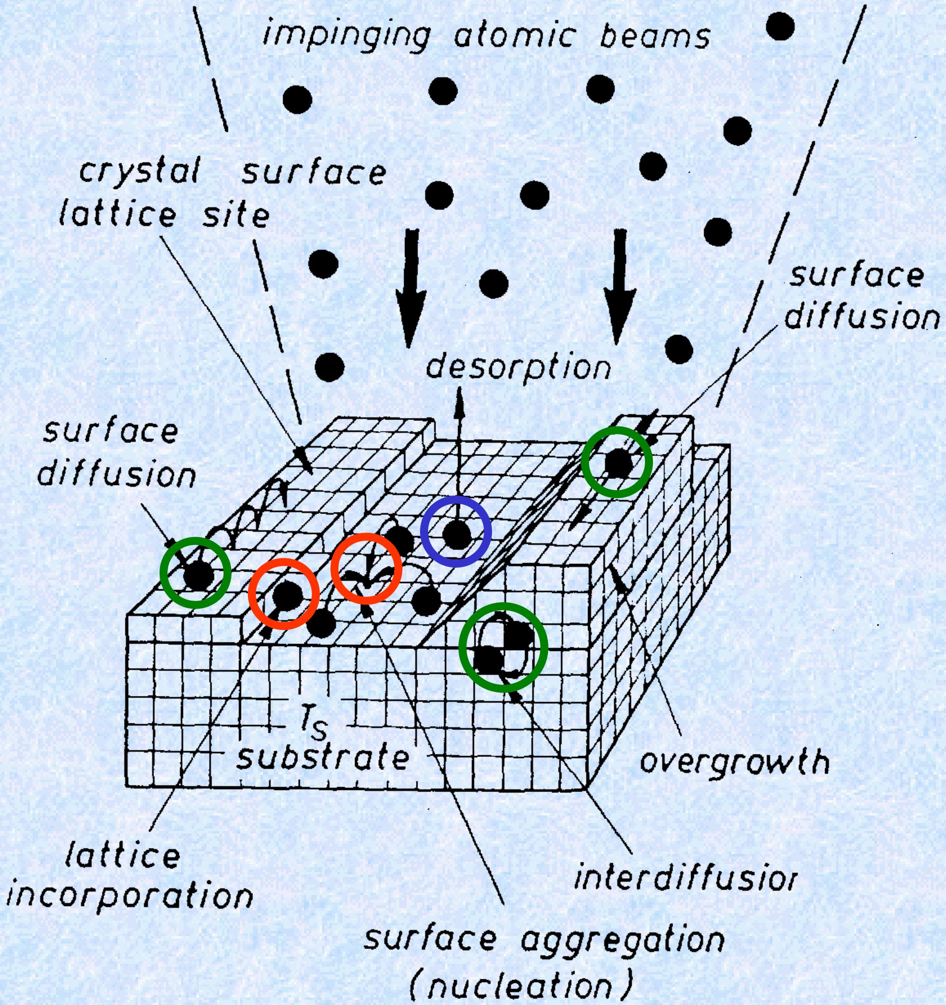

Positive Growth
- Incorporation into crystal steps
- Spontaneous nucleation

Negative Growth
- Desorption

Zero Growth
- Surface migration
- Interdiffusion

Elastically Strained Material

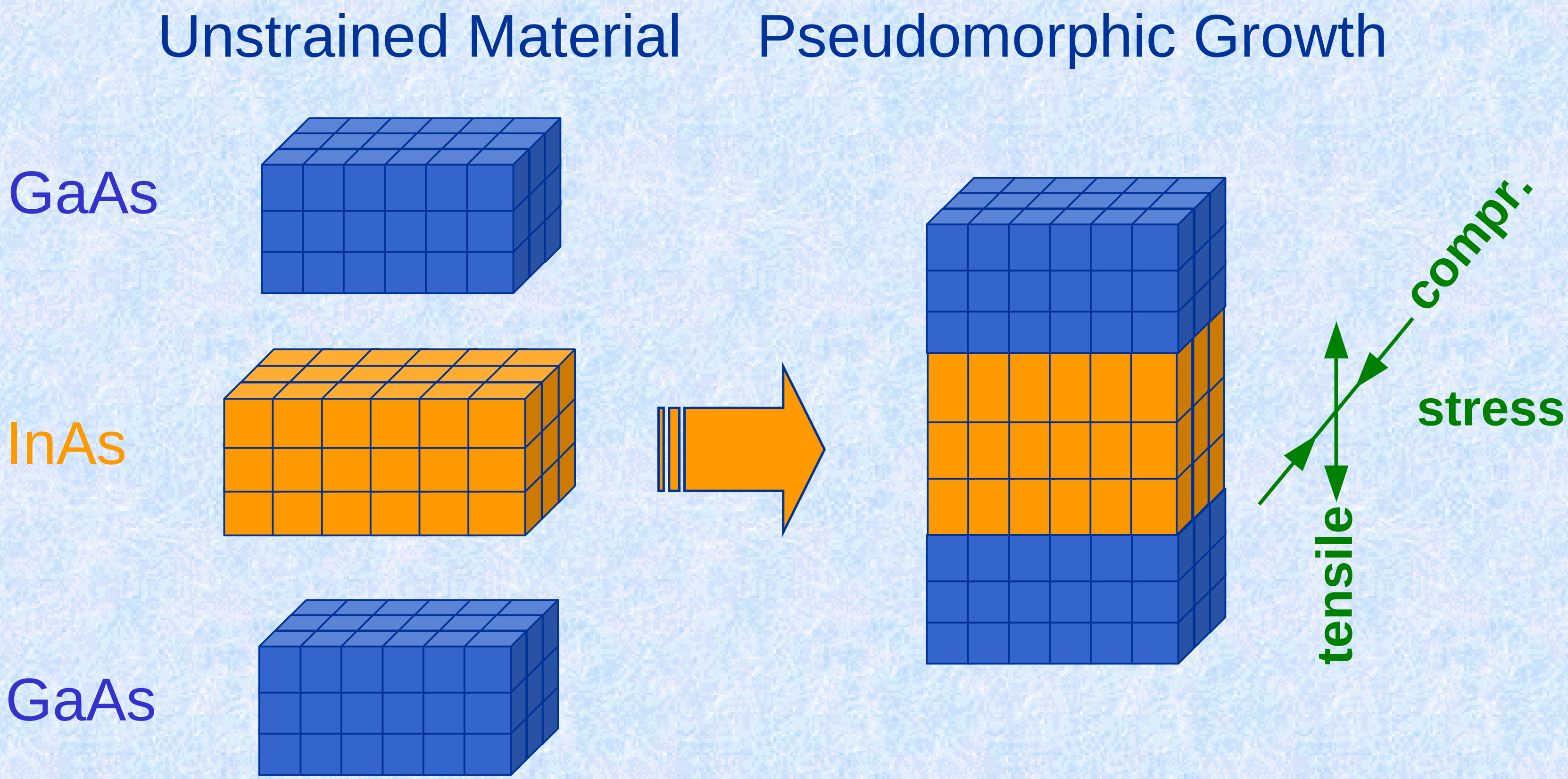

- InAs has 7.2 % larger lattice constant than GaAs
- For thin layers, growth without lattice defects possible

Self-Assembled Quantum Dot Growth

Strain driven self-organisation effect
(Stranski-Krastanov growth mode)

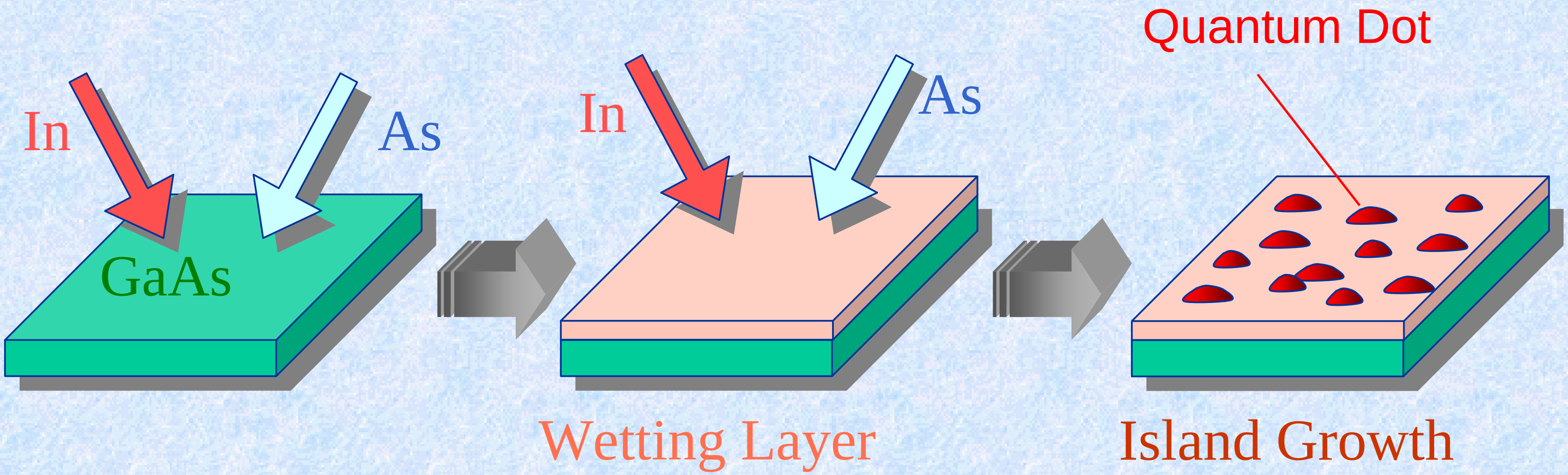

- Formation of atom-like islands (d ≈ 10-20 nm) due to energy minimation (wetting layer thickness: 1.7 ML for InAs)
- One dot contains still 10^5 atoms and behaves partially like bulk material (e.g., band structure properties)

Dot Nucleation Process

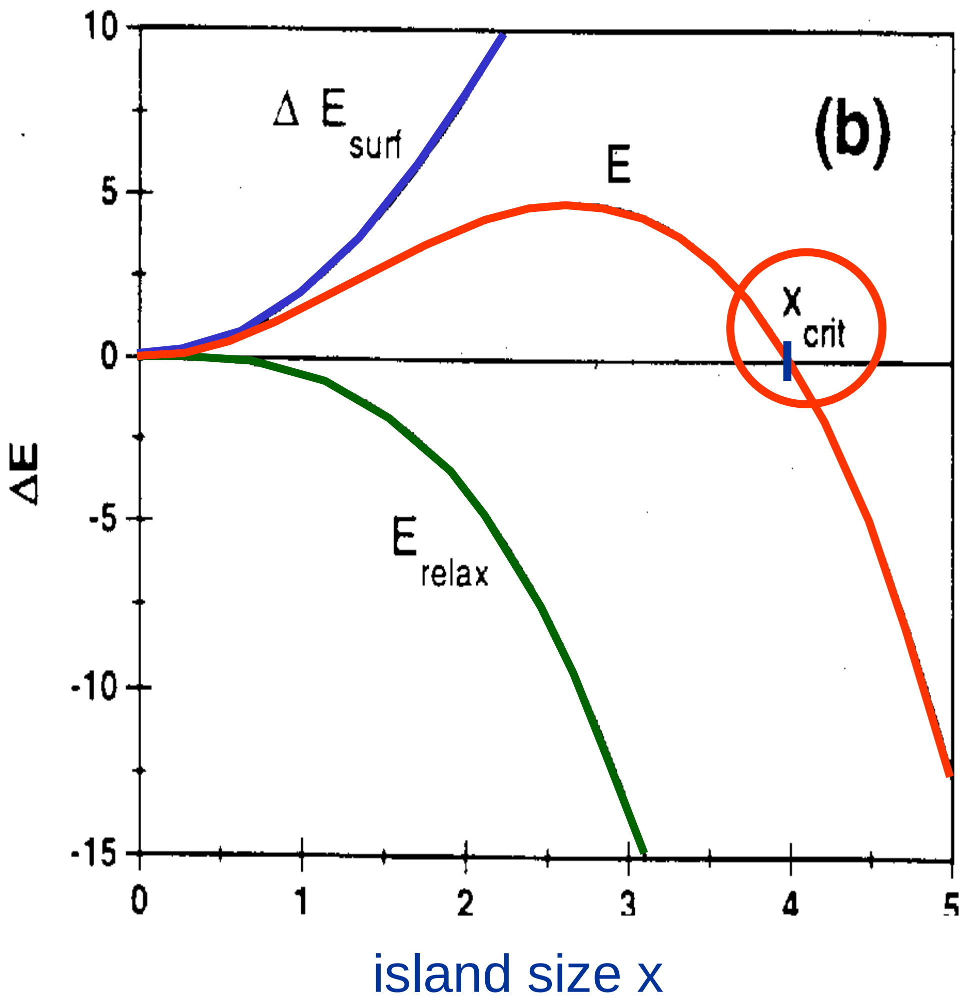

Surface energy difference:

$\Delta E_{surf} \sim x^2$ (~ surface)

Strain energy difference:

$\Delta E_{strain} \sim x^3$ (~ volume)

Energy balance:

$$\Delta E = C\gamma x^2 - \kappa\varepsilon^2 C' x^3$$

γ = surface energie,
κ = elasticity module,
ε = strain coefficient

→ **island formation:**
$x > x_{crit}$

InAs QD Formation on Different Substrates

InAs Quantum Dots
on GaAs

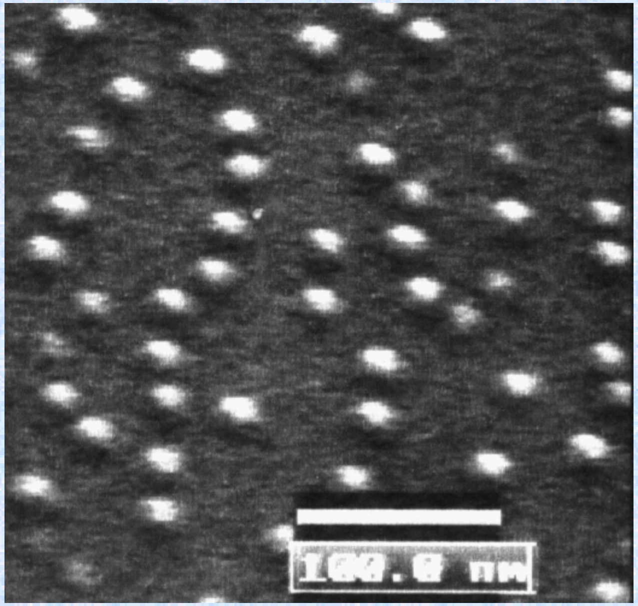

InAs Quantum Dashes
on AlGaInAs lattice
matched to InP

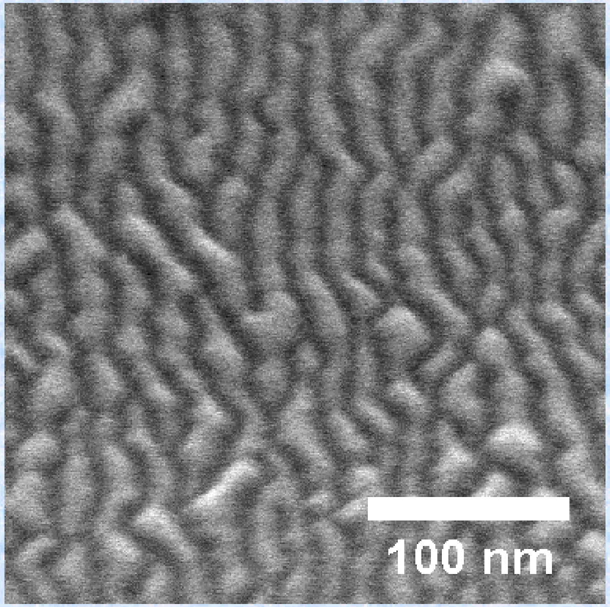

- QDash structures of high density are formed preferable in [0-11] crystal direction

Dot density control by growth temperature

- $In_{0.6}Ga_{0.4}As$ QDs with fundamental transitions energy of around 1.3 eV
- AFM images of uncovered quantum dots on GaAs surfaces

$T_{substrate}$ = 480 ℃

1x1µm

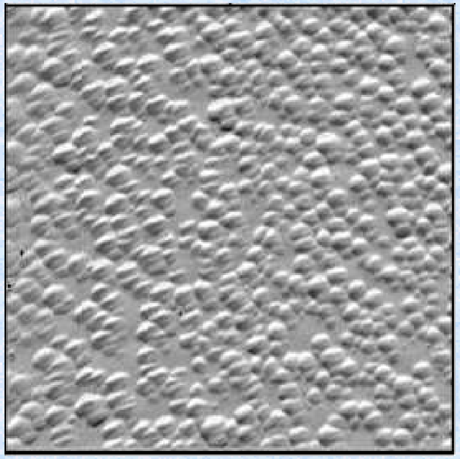

Dot density:

6 x 10^{10} cm^{-2}

$T_{substrate}$ = 510 ℃

1x1µm

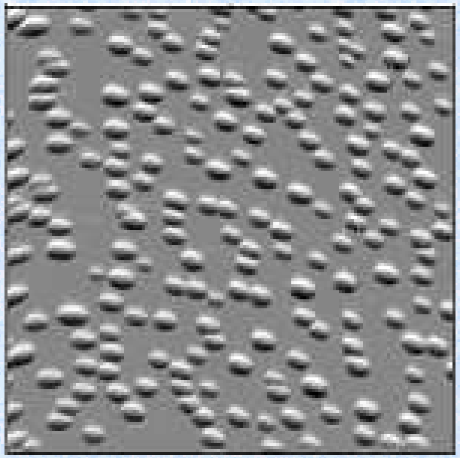

Dot density:

2 x 10^{10} cm^{-2}

$T_{substrate}$ = 530 ℃

1x1µm

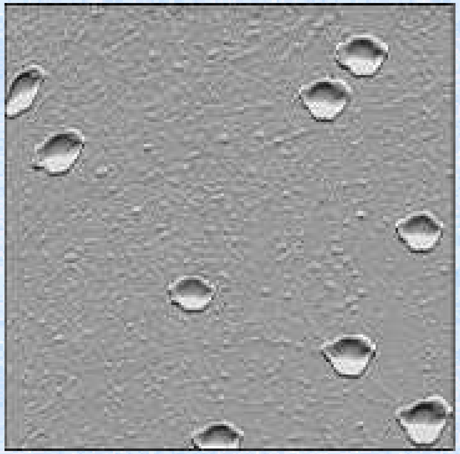

Dot density:

< 10^{9} cm^{-2}

Influence of In Concentration on Dot Shape

x_{In} = 60% x_{In} = 45% x_{In} = 30%

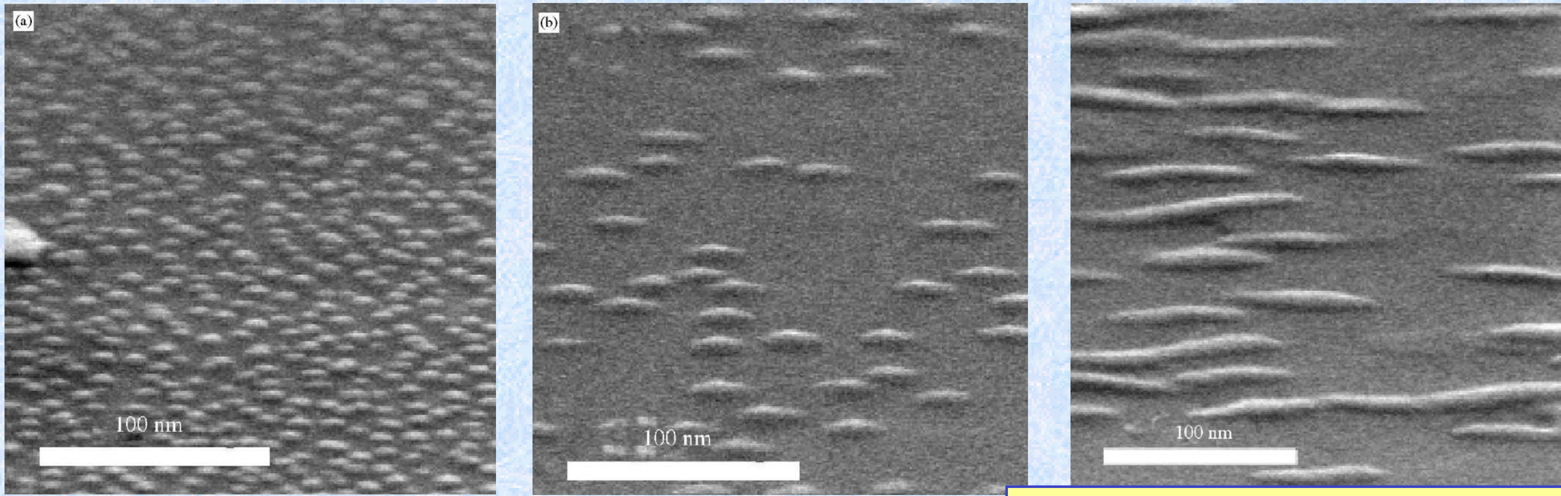

A. Löffler et al., JCG 286, 6 (2006)

x_{In} = 27% x_{In} = 30% x_{In} = 33%

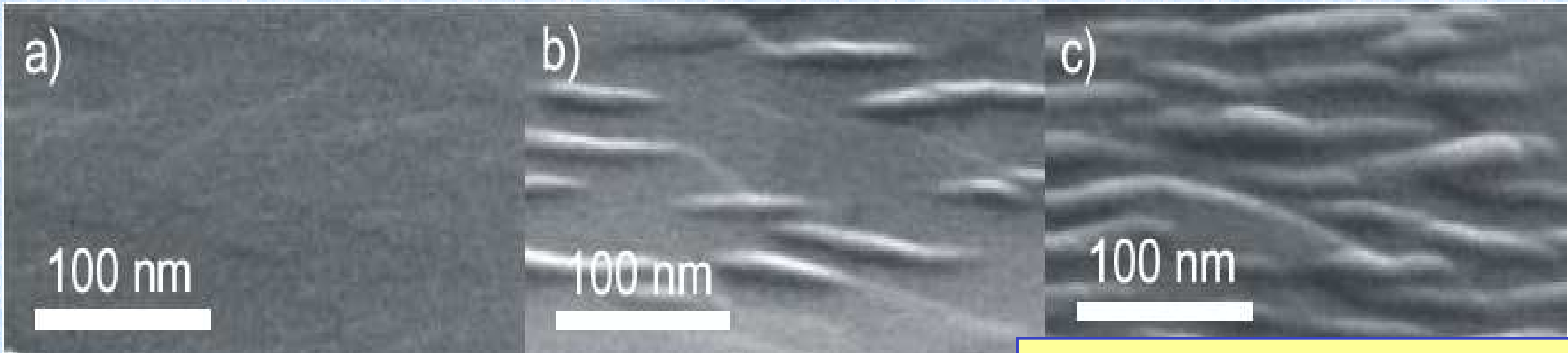

A. Löffler et al., PSS C 3, 3815 (2006)

Control of Dot Size by Layer Thickness

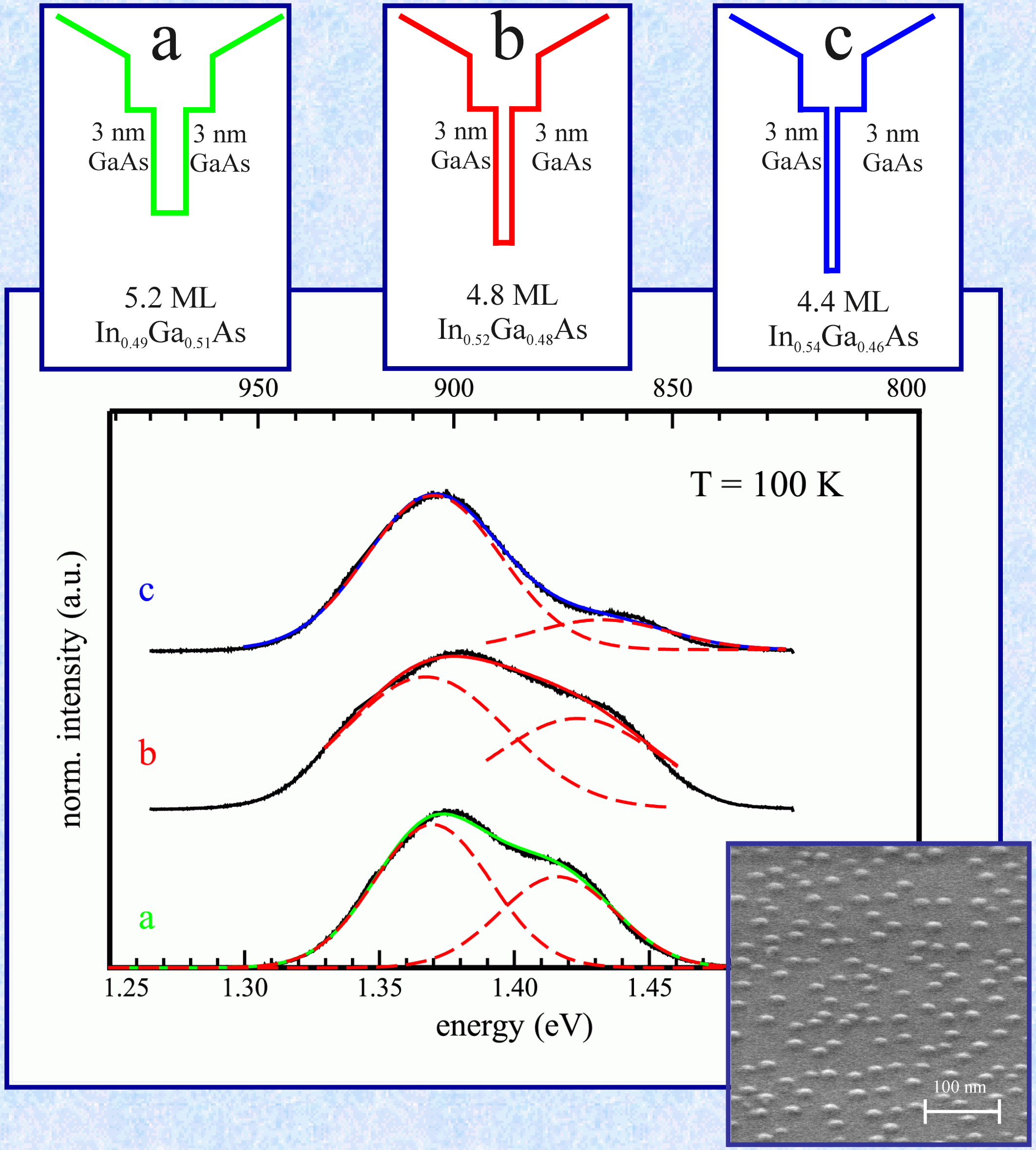

Photoluminescence measurement of different QD samples at high excitation powers:

energy separation between ground and first excited state increases with decreasing dot size:

a) $\Delta x \approx 47$ meV

b) $\Delta x \approx 56$ meV

c) $\Delta x \approx 65$ meV

⇒ **small QDs promising for tailoring gain spectrum of QD lasers**

J.P. Reithmaier et al.,
phys. stat. sol. B 234, 3981 (2006)

Strain Coupling

Preferential nu-
cleation of InAs
Aligned InAs Dot
Local Strain
InAs Dot

GaAs layer

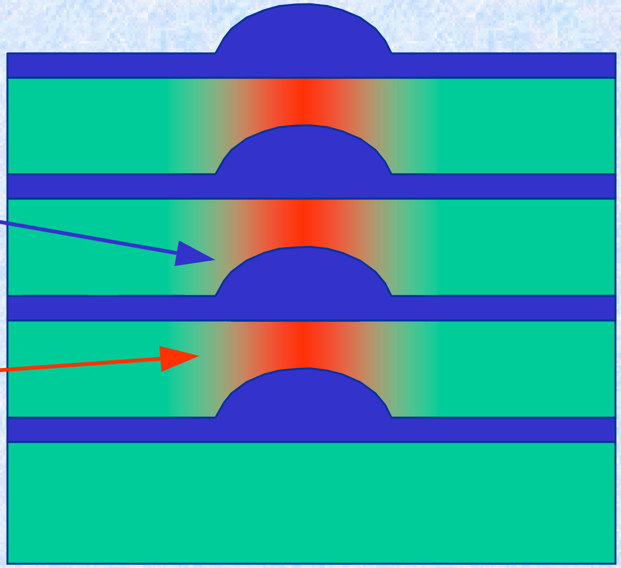

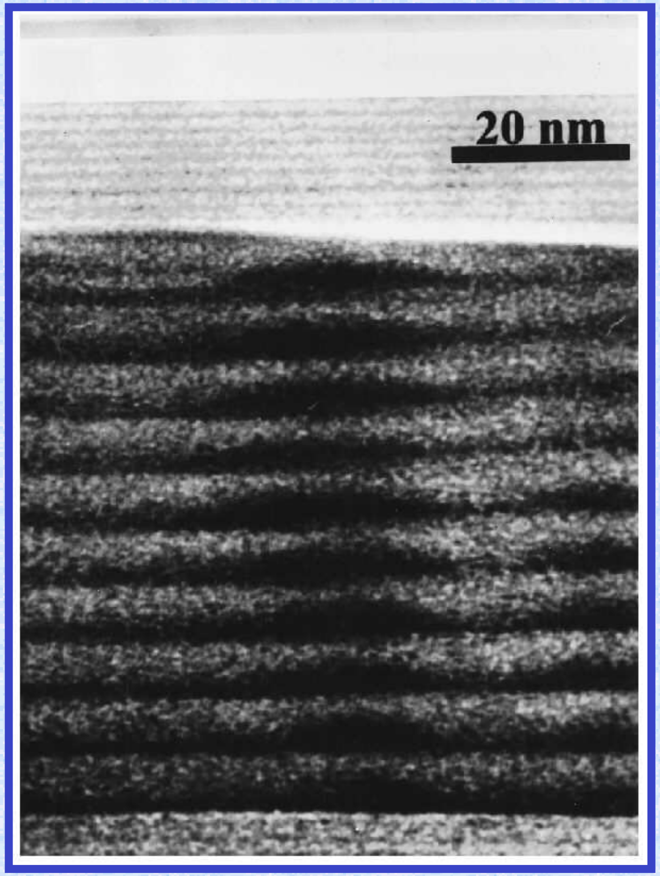

- Vertical alignment of QDs due to strain coupling
- Coupling strength dependent on thickness of GaAs intermediate layer (d < 30 nm)

Maximov et al., J. Appl. Phys. 83, 5561 (1998)

- Introduction and Some Basic Theory
  - density of states, gain function
  - dependence on dimensions
- Fabrication Technology
  - molecular beam epitaxy and Stranski-Krastanov growth mode
  - influence on geometry parameters
- Optical properties of real dots
  - single dot emission, higher order transitions
  - inhomogeneous linewidth, wetting layer
- Application examples of QD lasers
  - high power lasers (980 and 920 nm)
  - telecom lasers and amplifiers (1.3 and 1.55 µm)
  - single photon emitters and microcavity lasers

Potential shape of SA-QDots

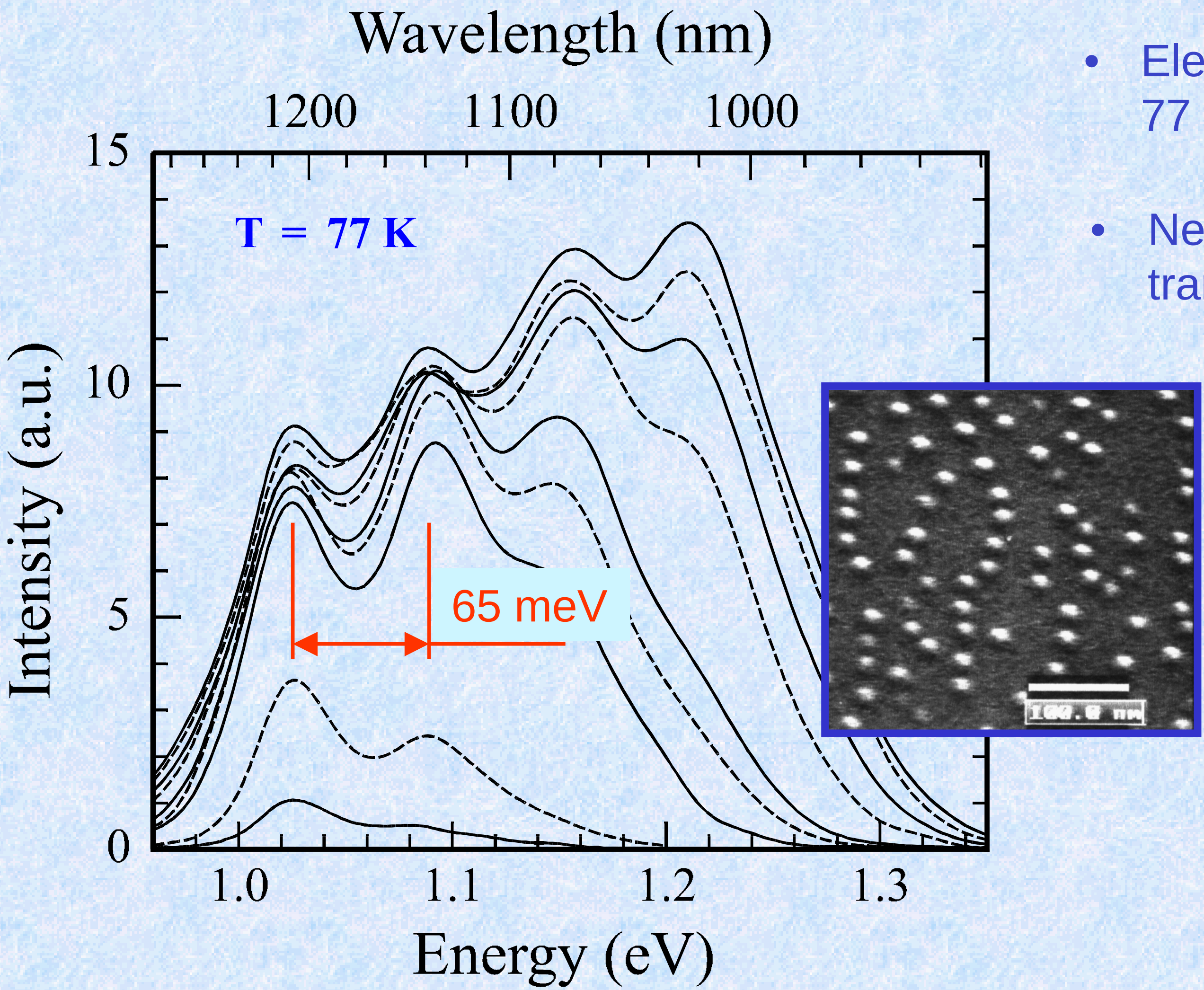

- Electroluminescence at 77 K
- Nearly equidistant transistion energies

→ Parabolic potential shape

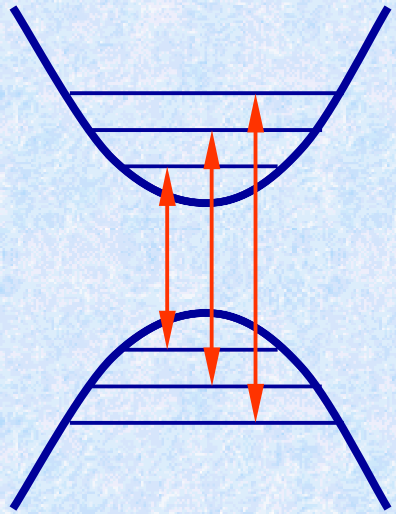

Quantum Dot Wavefunctions

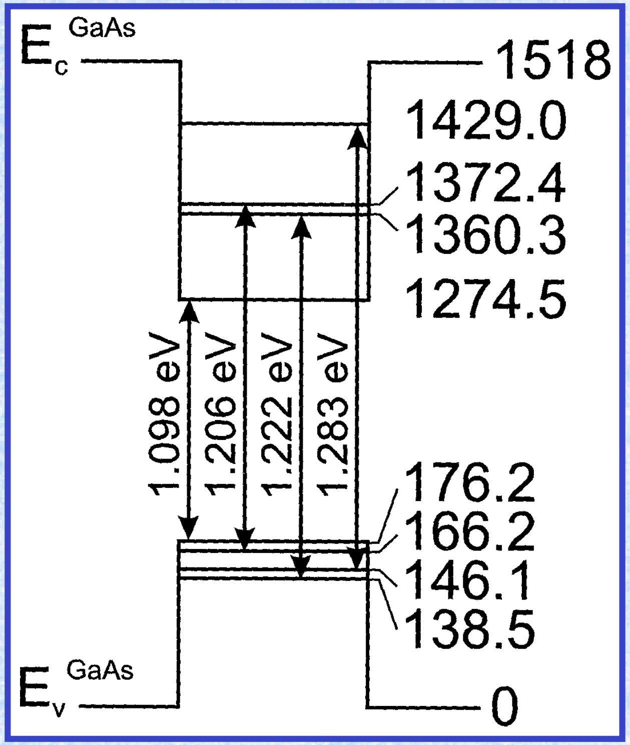

s and p type electron and hole states for an InAs/GaAs quantum dot (exciton formation is not taken into account).

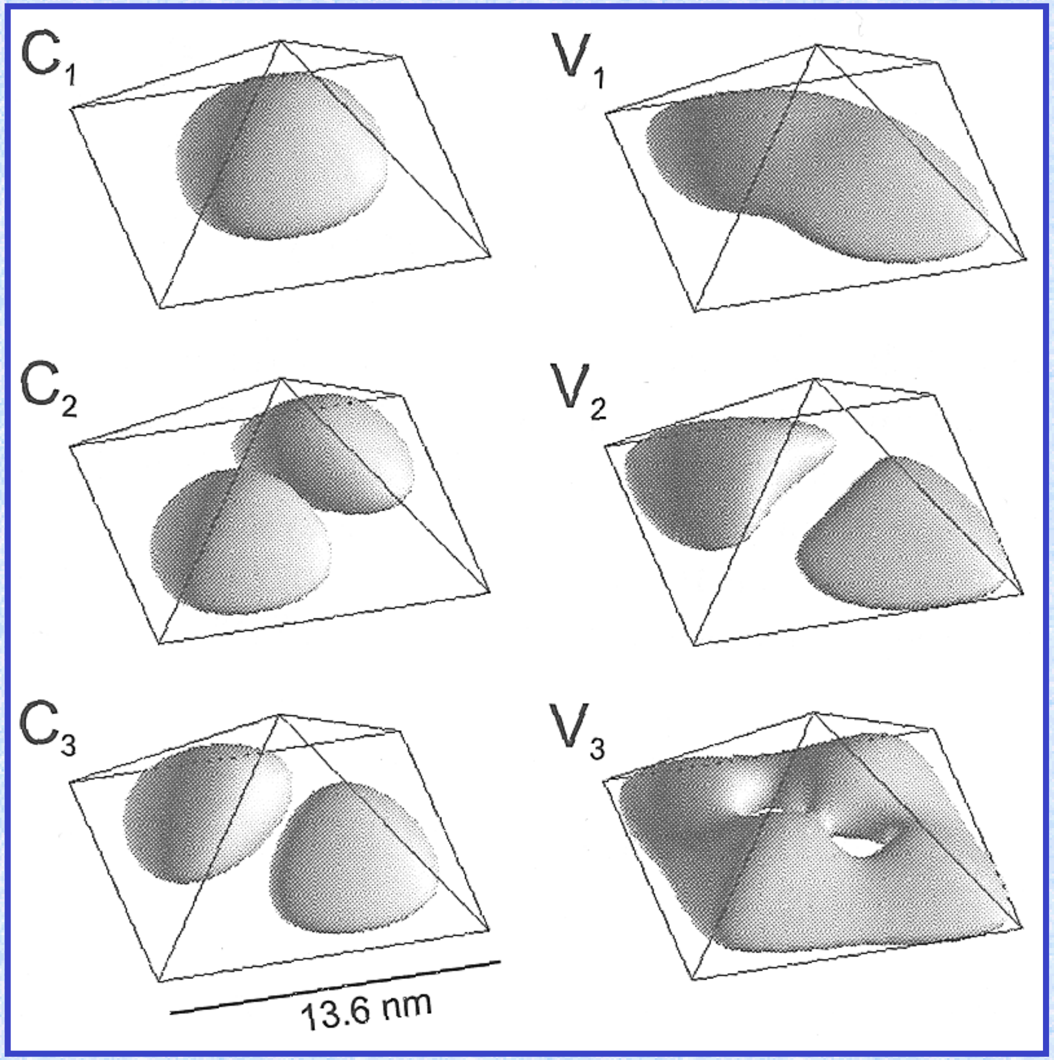

electron states

heavy hole states

D. Bimberg et al., "Quantum Dot Heterostructures", Wiley, 1999

Self-Assembled Quantum Dots

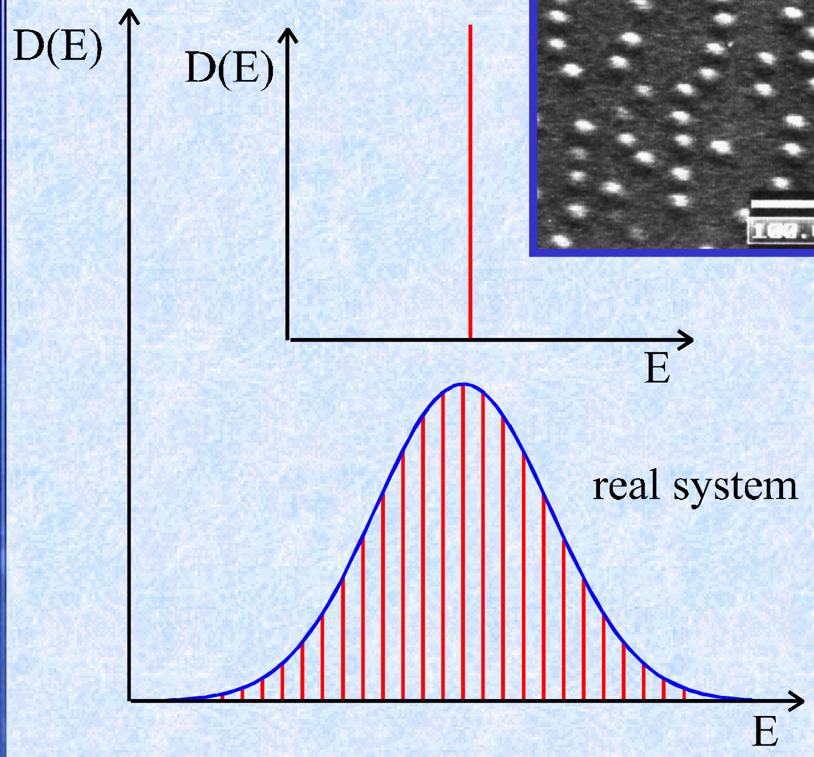

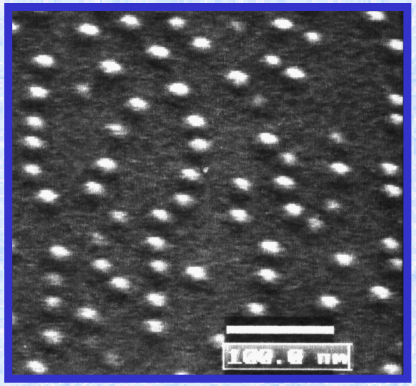

Single dot spectroscopy

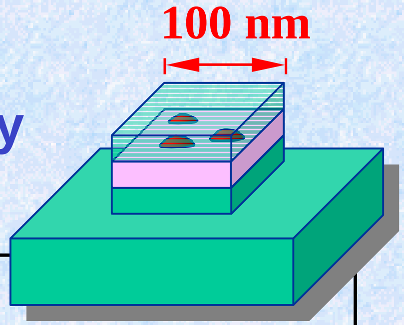

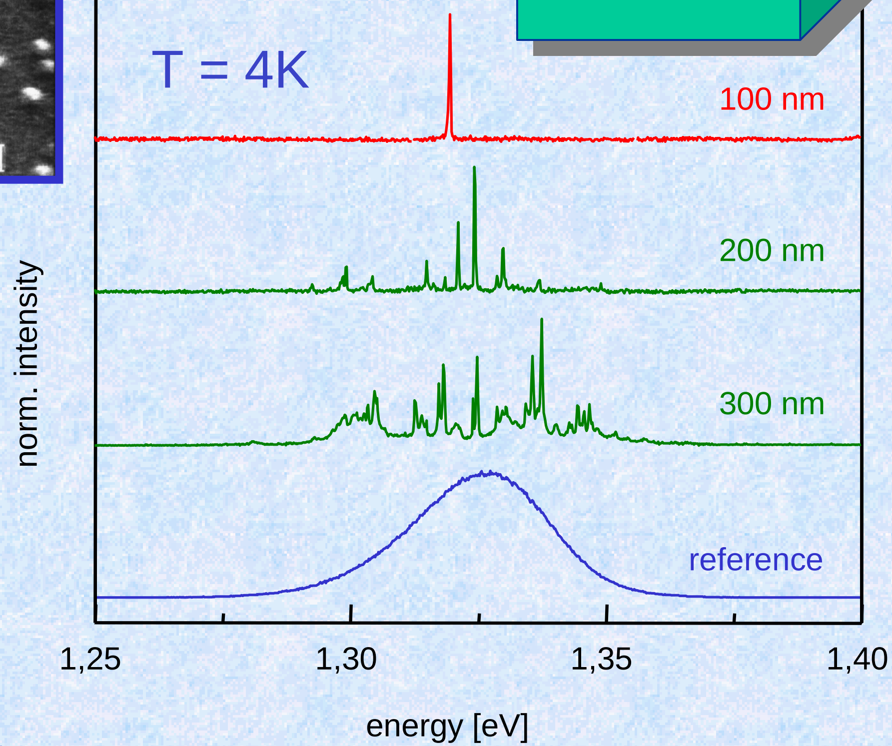

- Broad emissions spectrum of a dot ensemble due to size fluctuations
- Single line by dot selection

Spectrally Distributed Gain

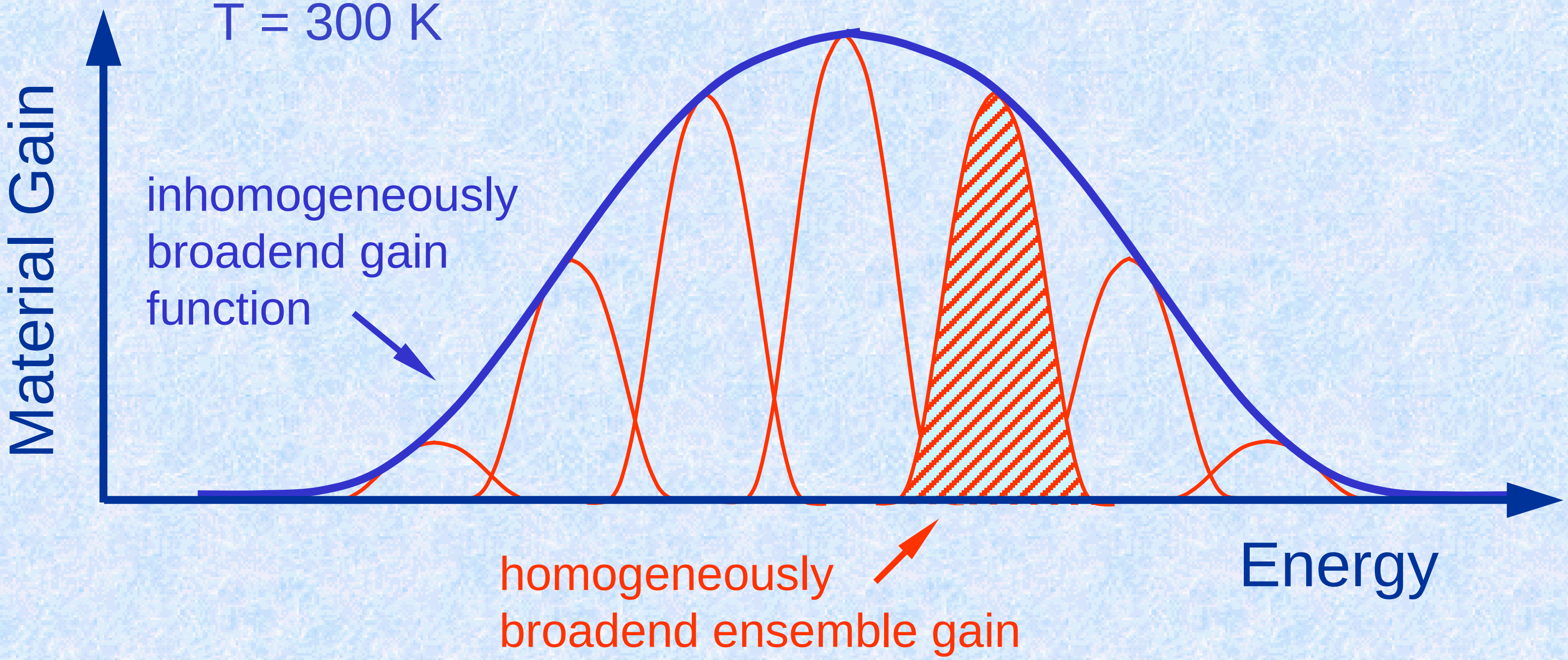

⇒ multi-wavelength amplification due to weak overlap between gain functions of different dot ensembles

homogeneous linewidth ≈ 5 - 10 meV (RT)

inhomogeneous linwidth ≈ 30 - 50 meV

Wetting layer thickness

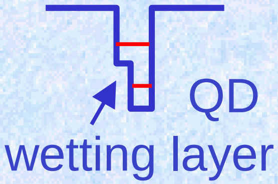

Photoreflectance spectroscopy

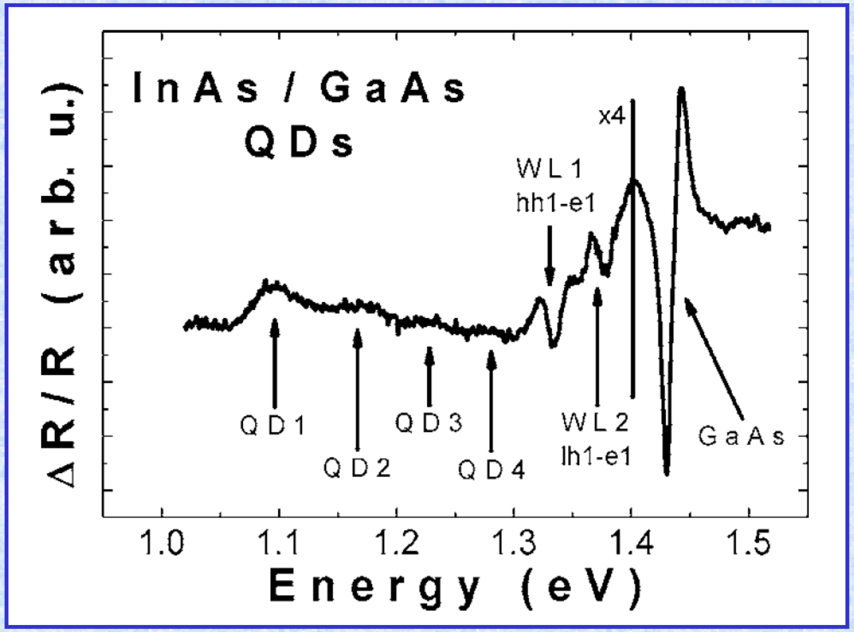

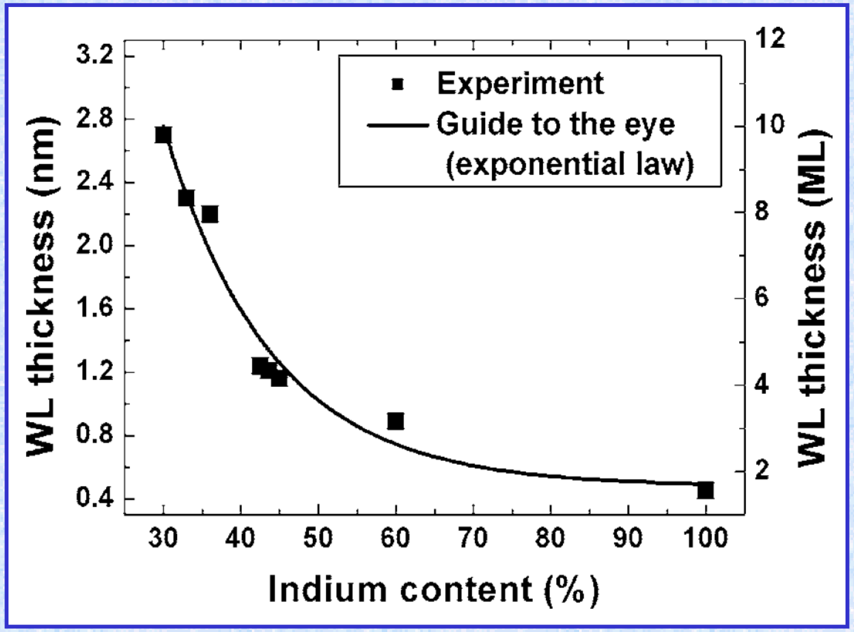

- Reflectance spectroscopy as very sensitive tool for optical transitions
- WL transitions clearly visible as hh_1-e_1 and lh_1-e_1 transitions
- WL transitions dependent on In concentration and thickness

- WL thickness varies from 1.6 ML (InAs) up to about 10 MLs ($In_{0.3}Ga_{0.7}As$)

G. Sek et al., JAP 100, 103529 (2006)

Gain Saturation and Flat Gain Profile

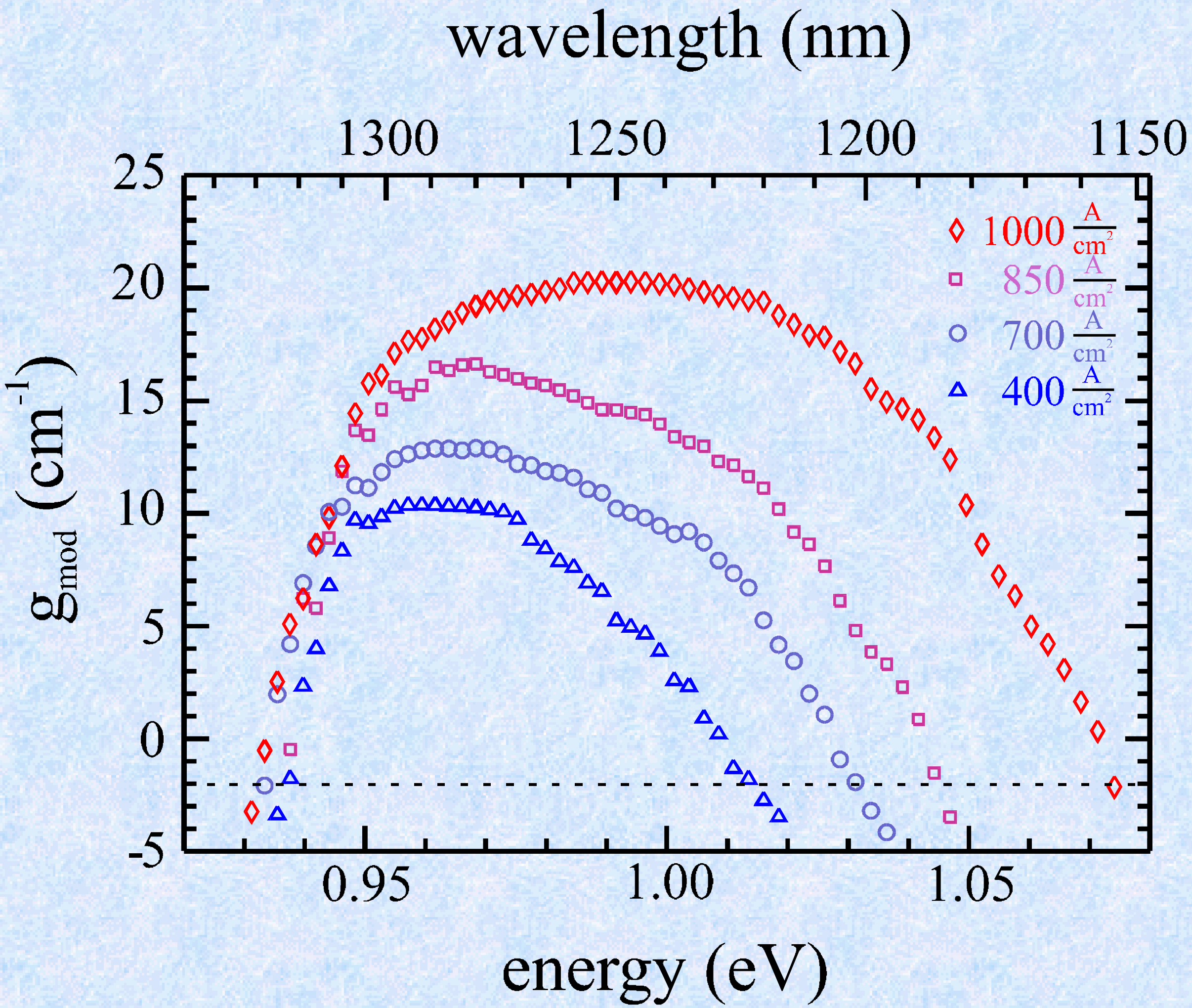

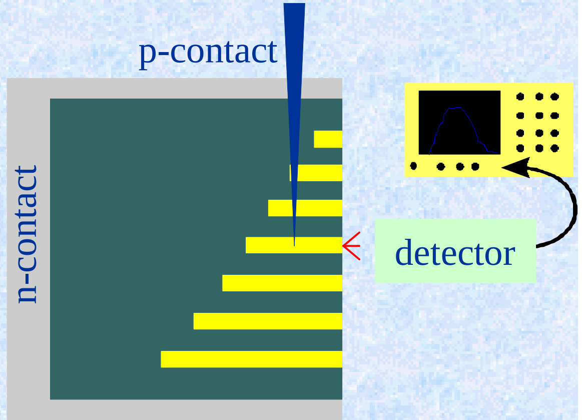

- High gain at transition energy already at low current density
- Fundamental transition saturates and higher order transitions contribute to the gain
- maximum gain of 17 - 20 cm^{-1} (6 dot layers stack)

→ suprisingly low modal gain of 3 cm^{-1} per dot layer

Auger Effect in Different Types of QDs

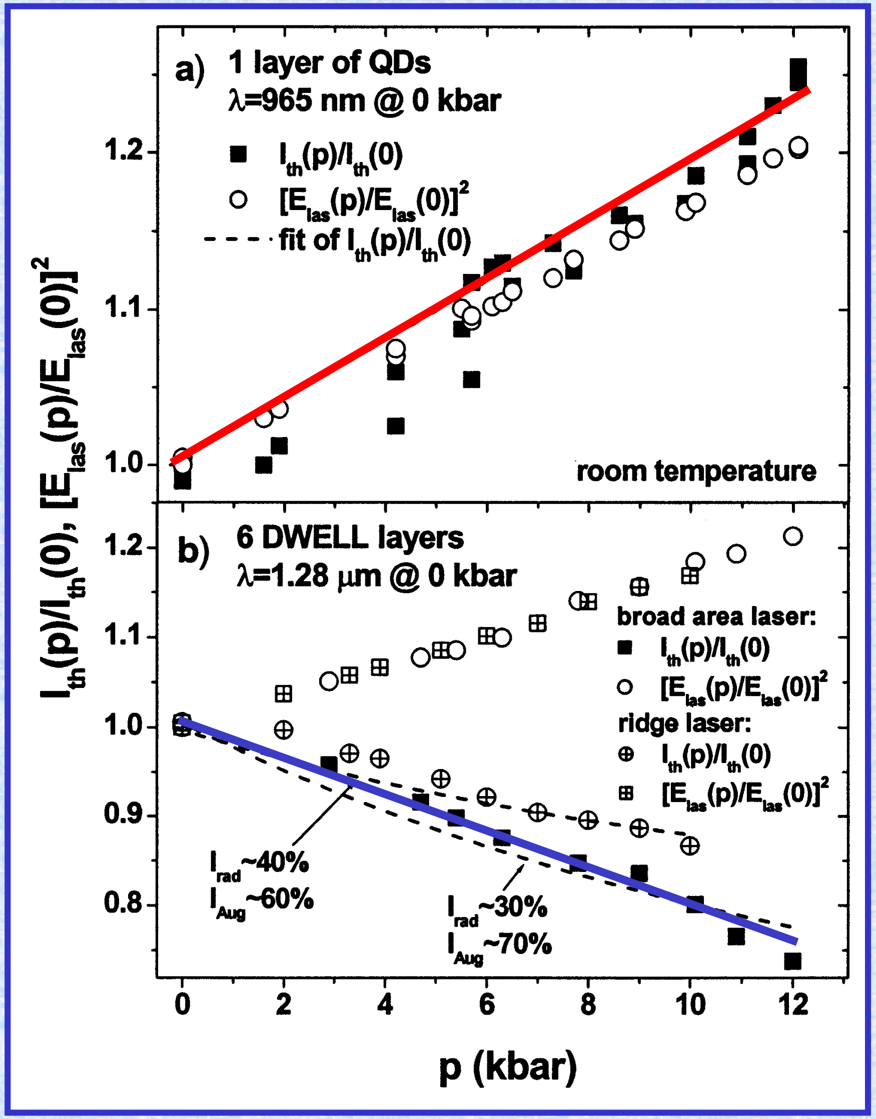

I.P. Marco et al., JSTQE 9, 1300 (2003)

- Hydrostatic pressure measurements show very different behavior of 980 nm and 1.3 µm QD lasers.
- I_{th}(980 nm) increases with p and E_{las} with p^2 as expected for radiative recombination
- I_{th}(1.3 µm) decreases by 26 % with p while E_{las} increases.

→ Behavior for 1.3 µm could be most likely explained by a significant contribution of Auger recombination as non-radiative process while 980 nm QD lasers seems to be dominated by radiative recombination.

Gain of 980 nm QD and QW-Laser

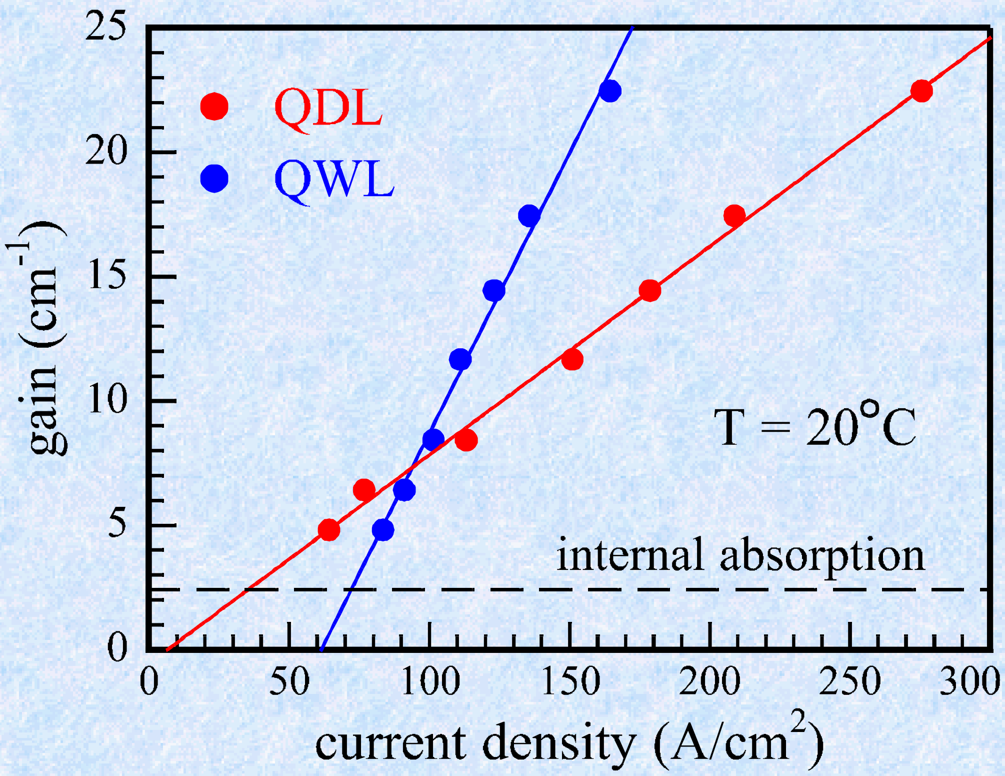

- Inversion condition already achieved at lower carrier densities
  $\rightarrow j_{tr}$ = 36 A/cm² (α_i = 2.2 cm^{-1})
  j_{th} = 54 A/cm² (2mm,HR/HR)
- Modal gain for single dot layer limited

$$\text{Threshold gain: } g_{th} = \alpha_i + \frac{1}{L}\ln\left(\frac{1}{\sqrt{R_1 R_2}}\right)$$

F. Klopf et al., APL 77, 1419 (2000)

- Introduction and Some Basic Theory
  - density of states, gain function
  - dependence on dimensions
- Fabrication Technology
  - molecular beam epitaxy and Stranski-Krastanov growth mode
  - influence on geometry parameters
- Optical properties of real dots
  - single dot emission, higher order transitions
  - inhomogeneous linewidth, wetting layer
- Application examples of QD lasers
  - high power lasers (980 / 920 nm)
  - ultra-broad band lasers (1.55 µm)
  - ultra-fast broadband SOAs (1.55 µm)

Motivation for Uncooled Pump Lasers

- Major costs in high power pump modules: Peltier cooler
- External wall plug efficiency of pump module dominated by Peltier cooler consumption.
- Strong cost reduction possible by passive cooling
- Passive cooling with QW laser impossible due to wavelength shift (> 20 nm between 0 – 65 ℃)
- 920 nm favourable due to broader absorption band
- High power 920 nm QD laser with temperature shift < 10 nm possible

Absorption spectrum of Yb fibre

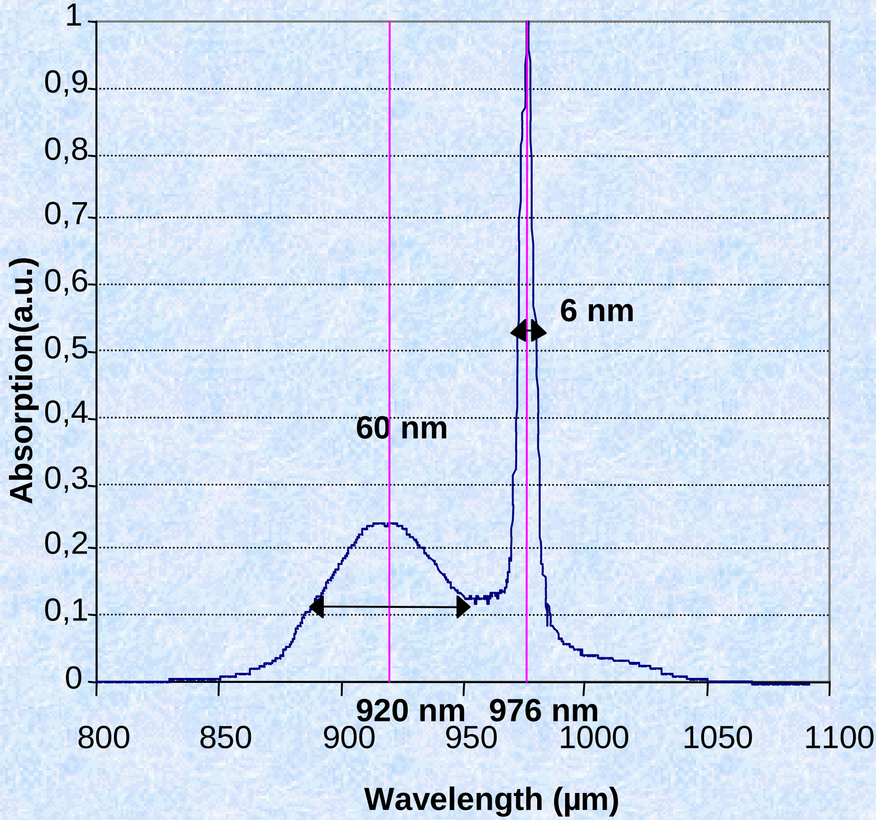

measured by Alcatel

High Power CW-Operation (980 nm laser)

FBH
Ferdinand-Braun-Institut für Höchstfrequenztechnik

- Epi-side down mounted devices mounted on heat sink
- P_{max} = 4.3 W (6.3 W) for 50 µm (100 µm) stripe width in cw
- Record in cw output power and power per stripe width (86 mW/µm)
- P_{max} = 5.4 W (9.5 W) for 50 µm (100 µm) stripe width in qcw (100 µs pulses) → (104 mW/µm)

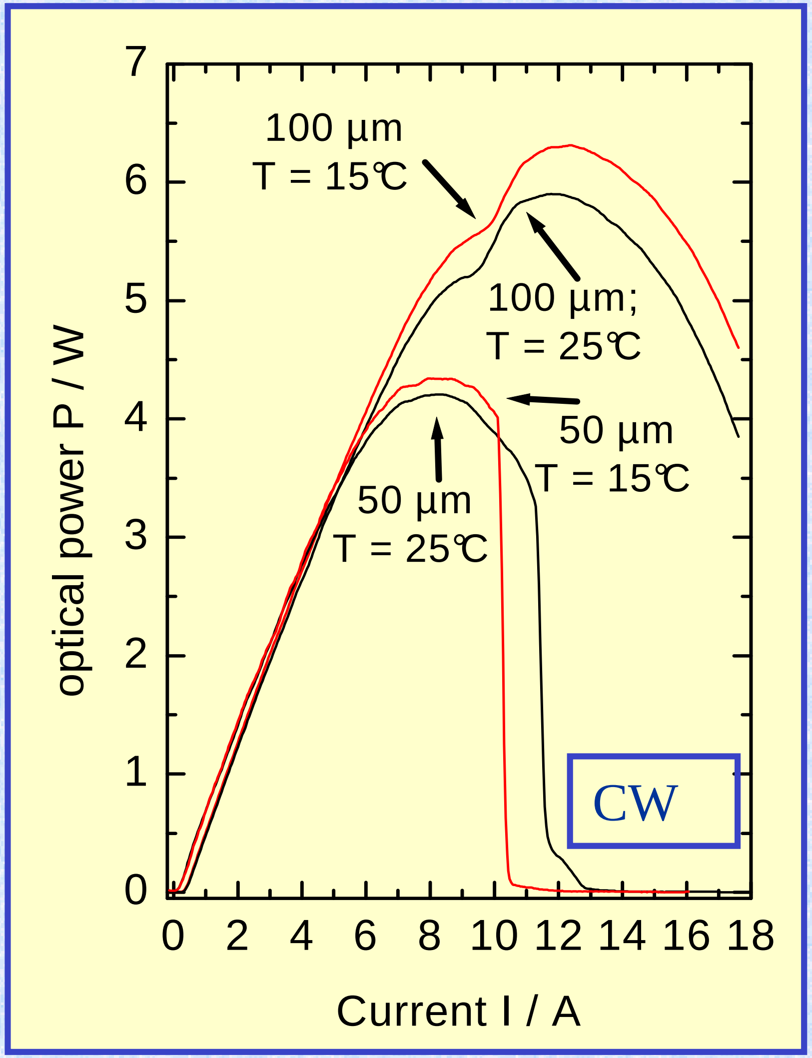

B. Sumpf et al., EL 39, 1655 (2003)

High Power Lifetime Measurements (980 nm)

FBH
Ferdinand-Braun-Institut für Höchstfrequenztechnik

- Epi-side down mounted devices
- 1 mm long, 70 µm wide stripes
- 2300 h without failures
- > 1000 h at 2 W (≈ 30 mW/µm)

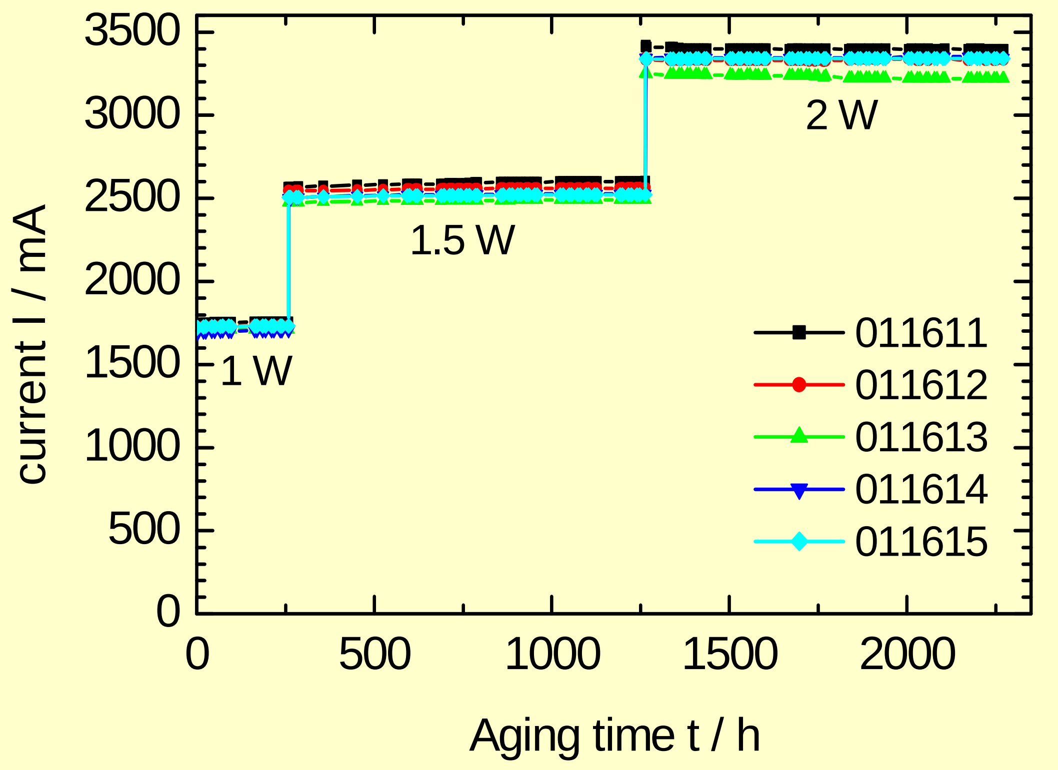

Temperature Stability of Wavelength (980 nm)

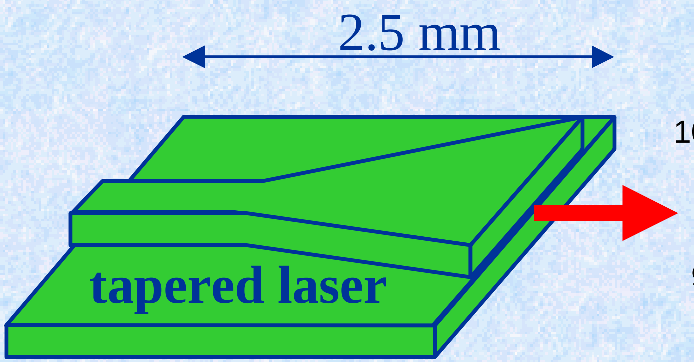

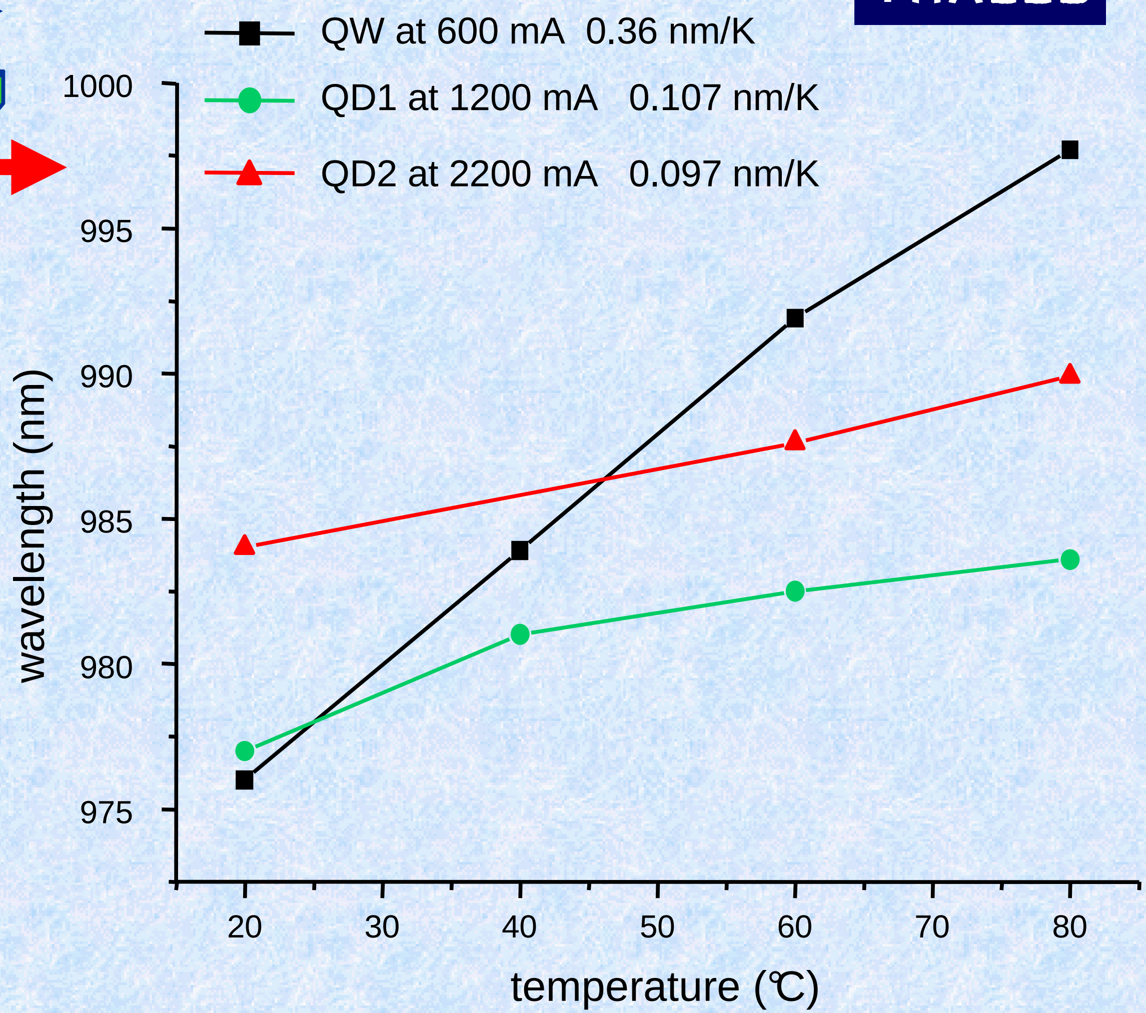

- Very low temperature dependence for QD lasers
- Between 20 – 80℃
  QW: Δλ = 22 nm
  QD: Δλ < 6 nm

S.C. Auzanneau et al., APL 84, 2238 (2004)

High Power Measurement Data of 920 nm QD Lasers

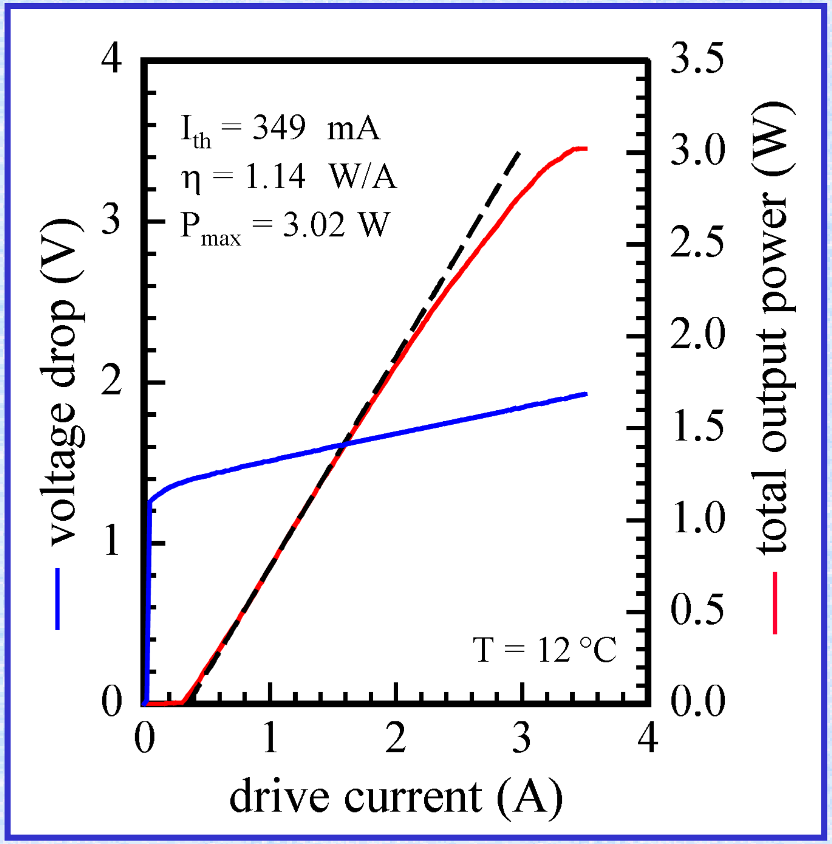

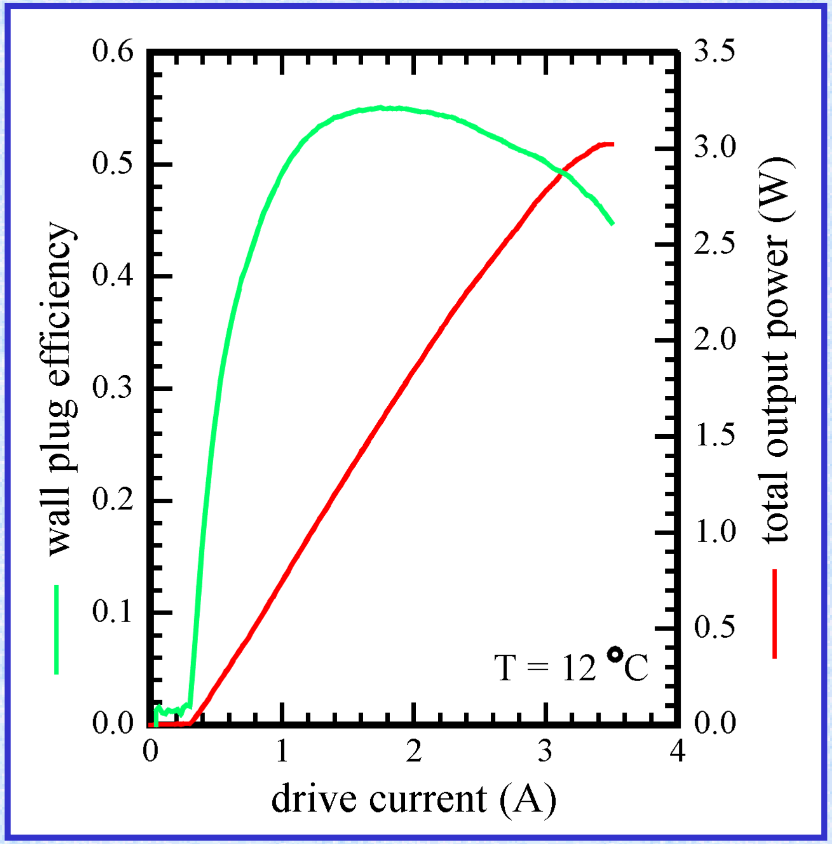

As-cleaved device,
1 mm long, 100 µm wide

Wall-plug efficiency of 55 % at 1.5 W

S. Deubert et al, EL 41, 1125 (2005)

Temperature Stability of Laser Performance (920 nm)

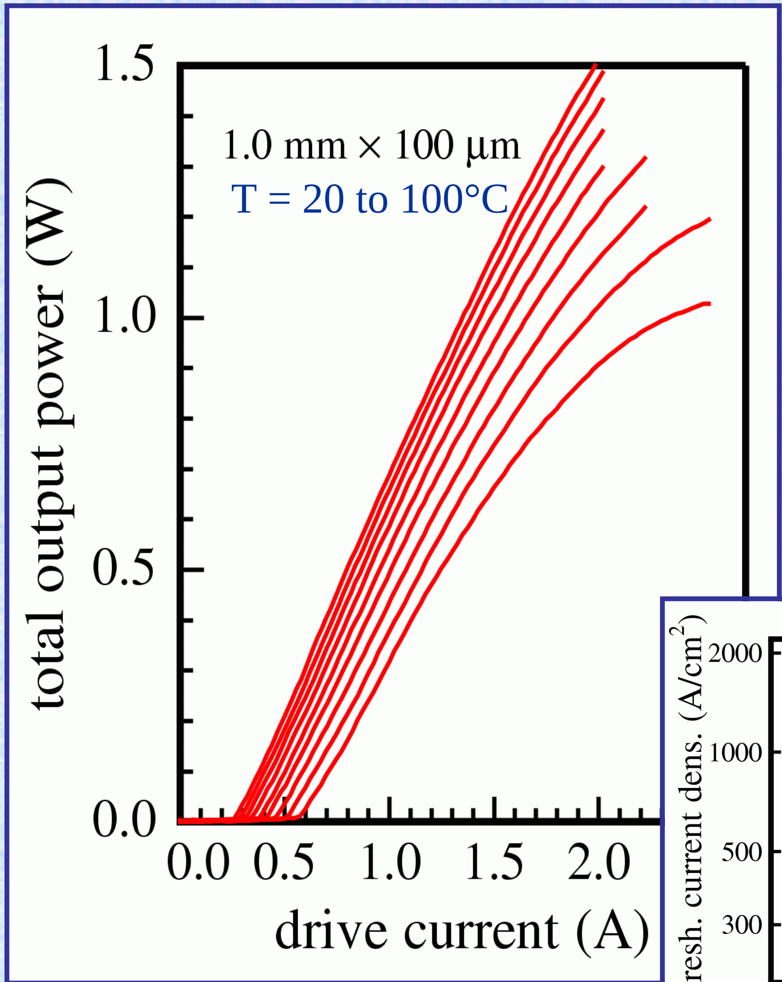

CW operation of a 1.0 mm × 100 µm:

- Temperature from 20 to 100℃ in steps of 10℃
- High temperature stability of threshold and efficiency
- Emission wavelength at about 915 nm
- Output power of P > 1 W @ 100℃

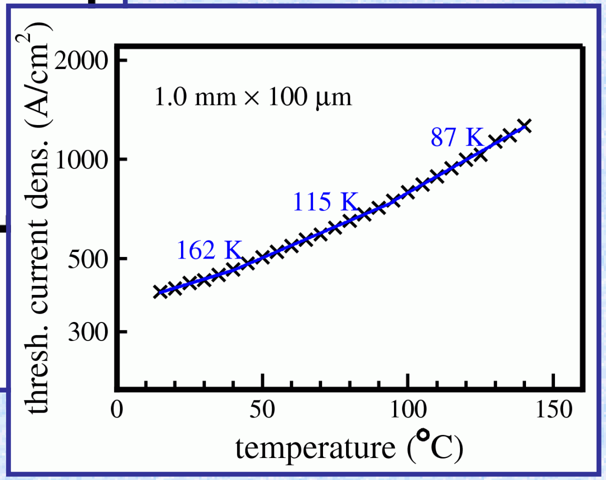

Pulsed operation

- T_{max} > 140 ℃
- High T_0 of 162 K up to 40 ℃ and > 150K up to 60℃

920 nm Tapered QD Lasers

Würzburg University
Micro Structure Laboratory

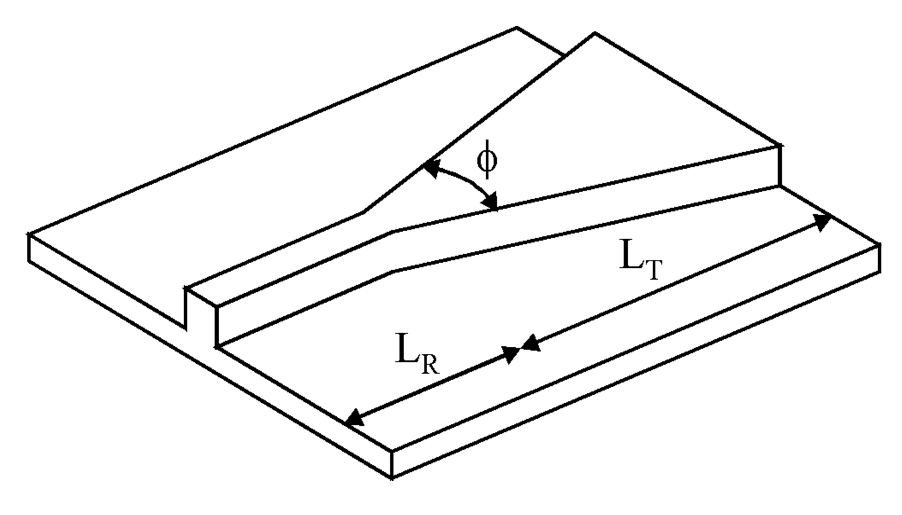

Near field intensity profile at P_{cw} = 1 W

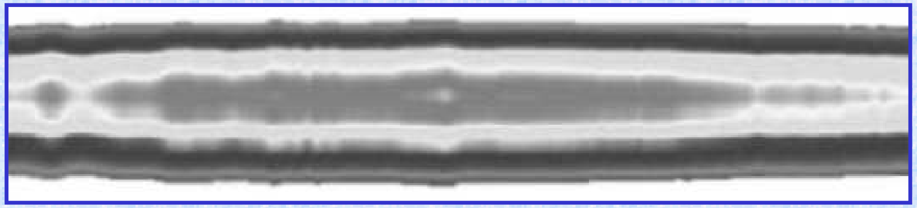

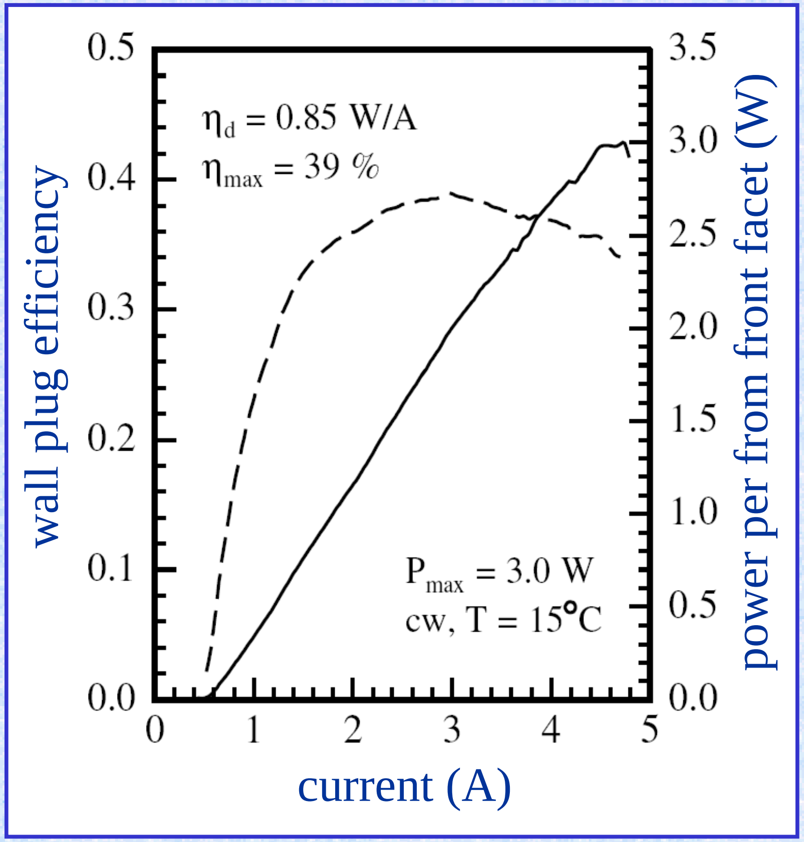

- High single lobe output power
- M^2 = 2.4 at 1 W output power
- About 4 times higher brilliance than BA-lasers (50 $MWcm^{-2}sr^{-1}$)

- Tapered lasers with L_R = 1 mm, L_T = 2 mm, ϕ = 6°
- P_{max} = 3W, wall plug eff. up to 39%

W. Kaiser et al, to be published

Single Mode QD Tapered Lasers (920 nm)

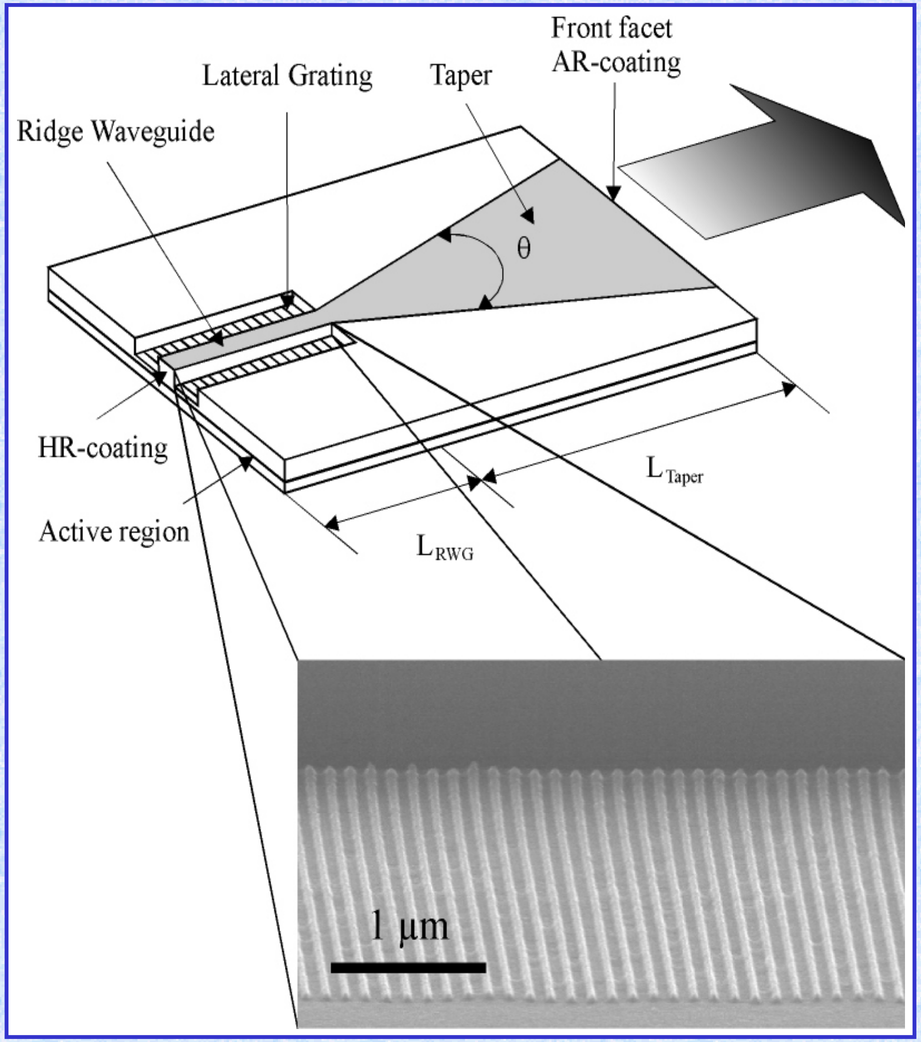

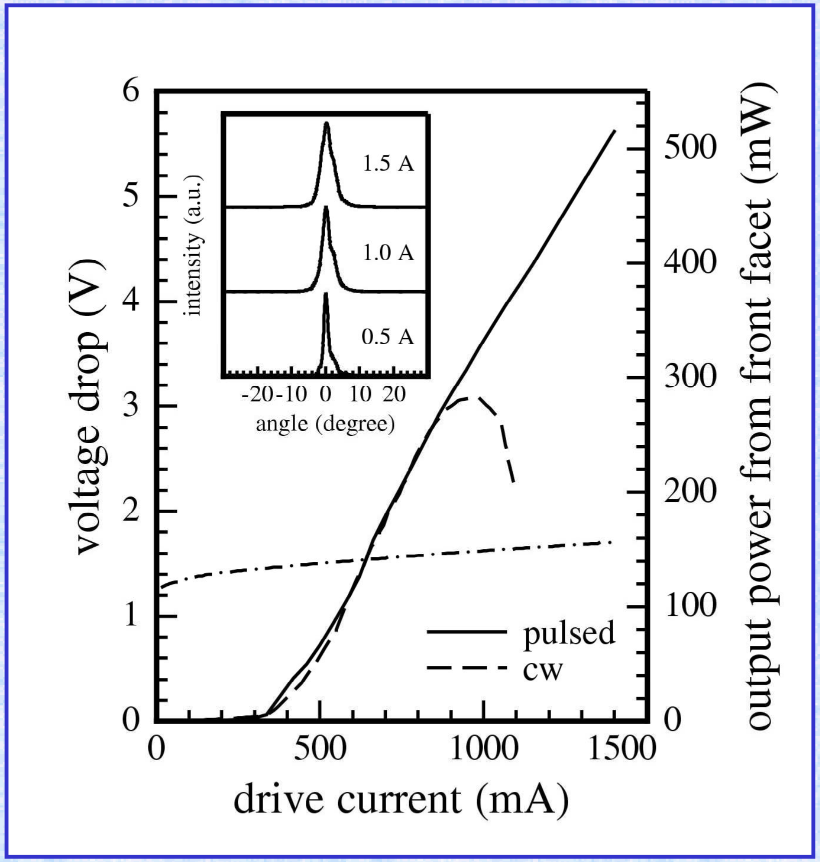

- Lateral gratings fix emission wavelength
- Single mode emission up to 500 mW

W. Kaiser et al, to be published

Wavelength Stabilized QD Lasers with Gratings

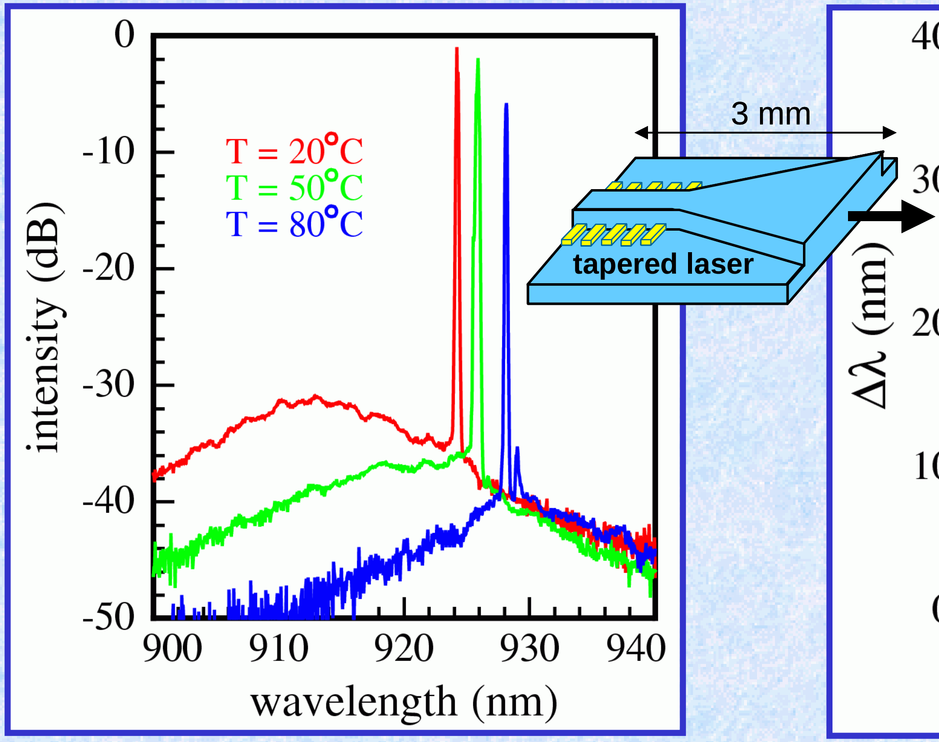

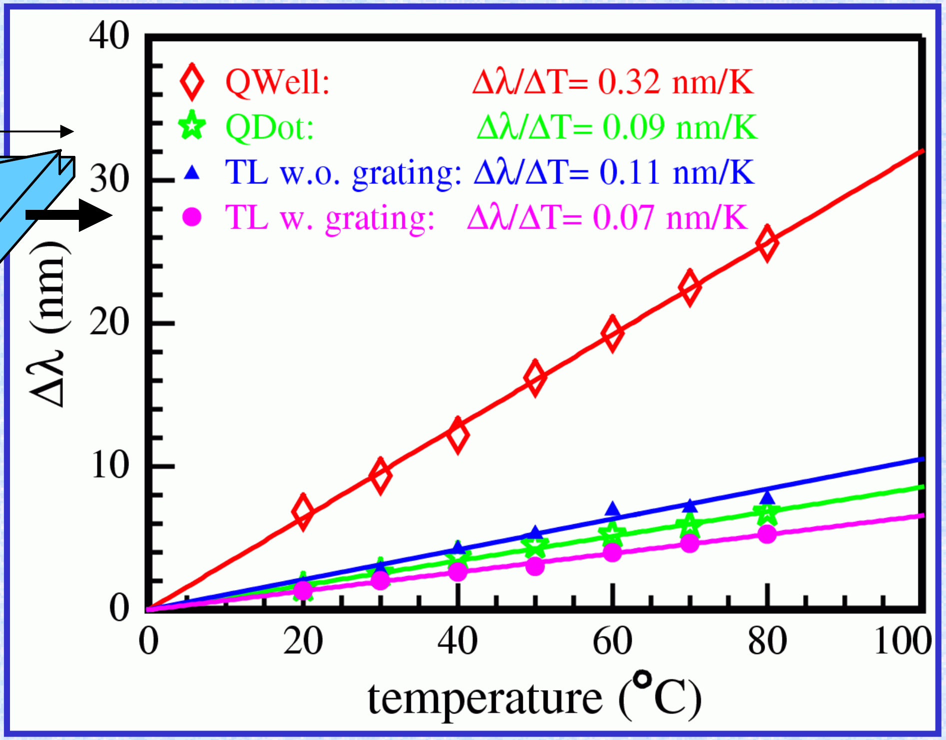

- Tapered lasers with lateral gratings
- Single mode emission between 20 to 80 °C due to temperature insensitive gain function
- Temperature stable emission wavelength (0.07 nm/K)
- Temperature dependence of QD material at same order than refractive index change

Kaiser et al., CLEO, Long Beach (May, 2005)

Temperature Stable Laser Performance (920 nm)

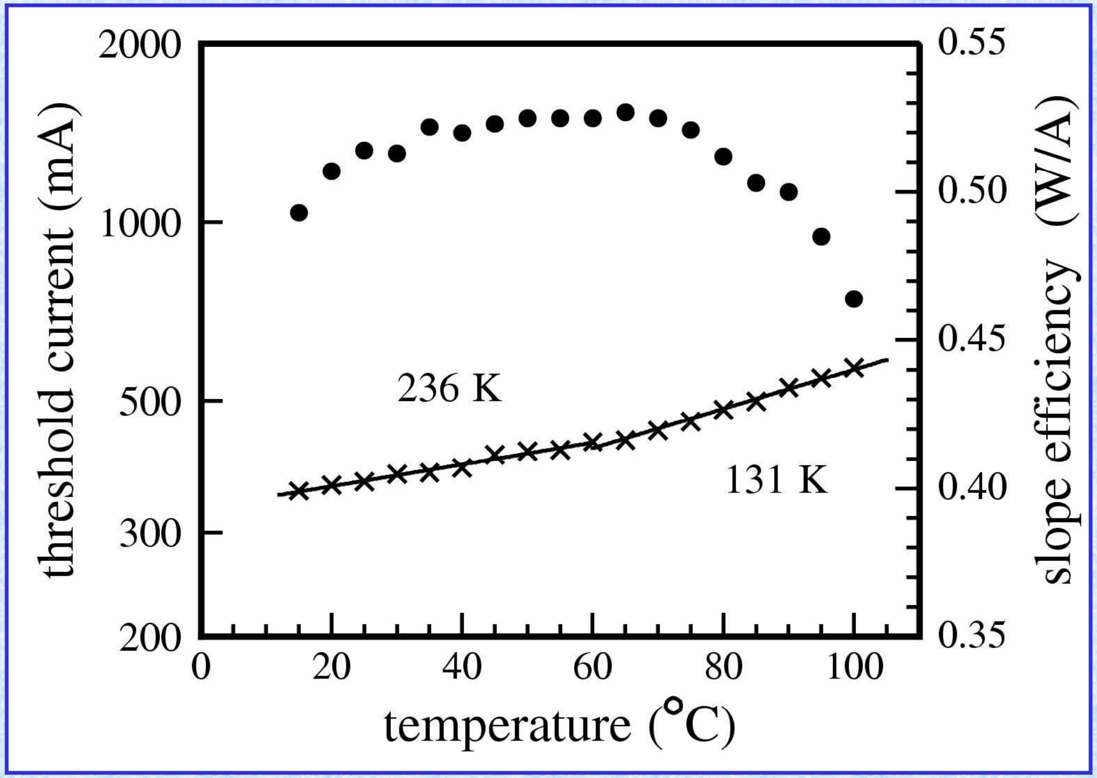

- Constant slope efficiency between 20 – 80 °C
- High T_0 value up to operation temperatures of 100 °C
- Improvement also due to nearly coincident temperature development of gain and grating period

W. Kaiser et al, to be published

- Introduction and Some Basic Theory
  - density of states, gain function
  - dependence on dimensions

- Fabrication Technology
  - molecular beam epitaxy and Stranski-Krastanov growth mode
  - influence on geometry parameters

- Optical properties of real dots
  - single dot emission, higher order transitions
  - inhomogeneous linewidth, wetting layer

- Application examples of QD lasers
  - high power lasers (980 / 920 nm)
  - ultra-broad band lasers (1.55 µm)
  - ultra-fast broadband SOAs (1.55 µm)

QDashes on (001) InP-Substrates

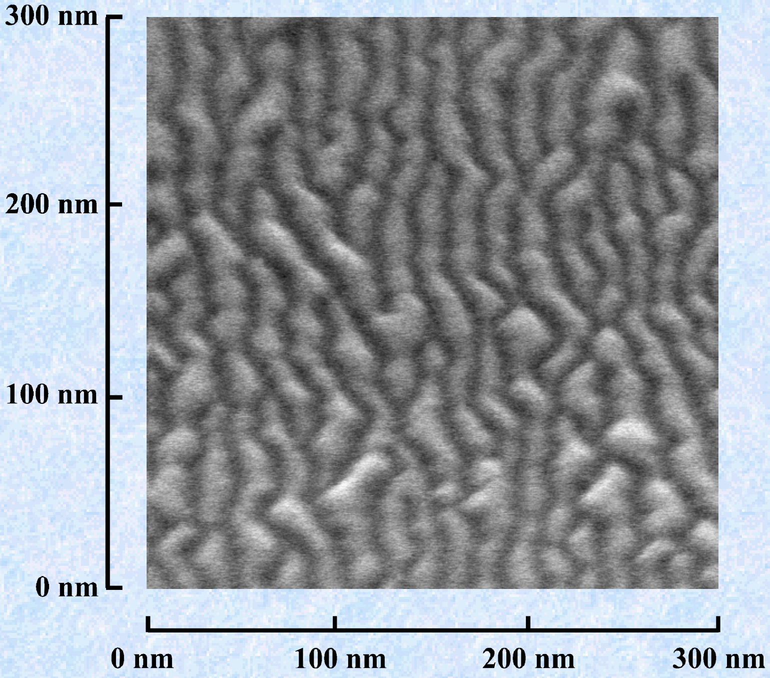

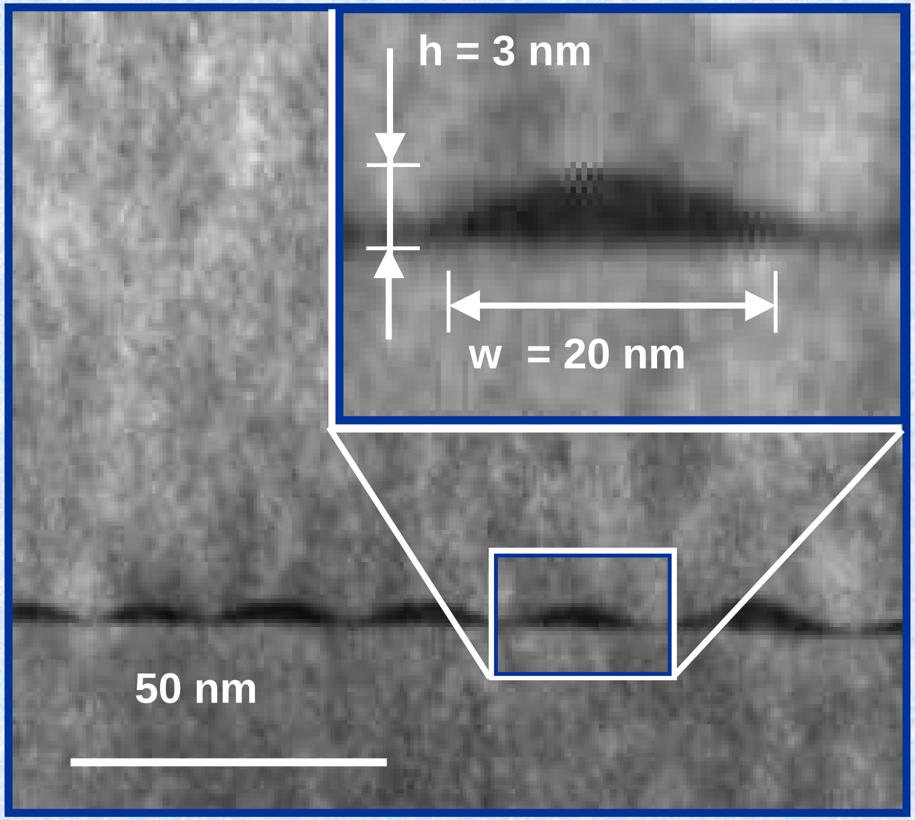

- XTEM images done by Univ. of Duisburg (T. Kümmell, G. Bacher)
- Pyramidal like cross-section with dominating vertical quantization

T. Kümmell et al., APL 86, 253112 (2005)

Shape Preserving QDash Formation Process

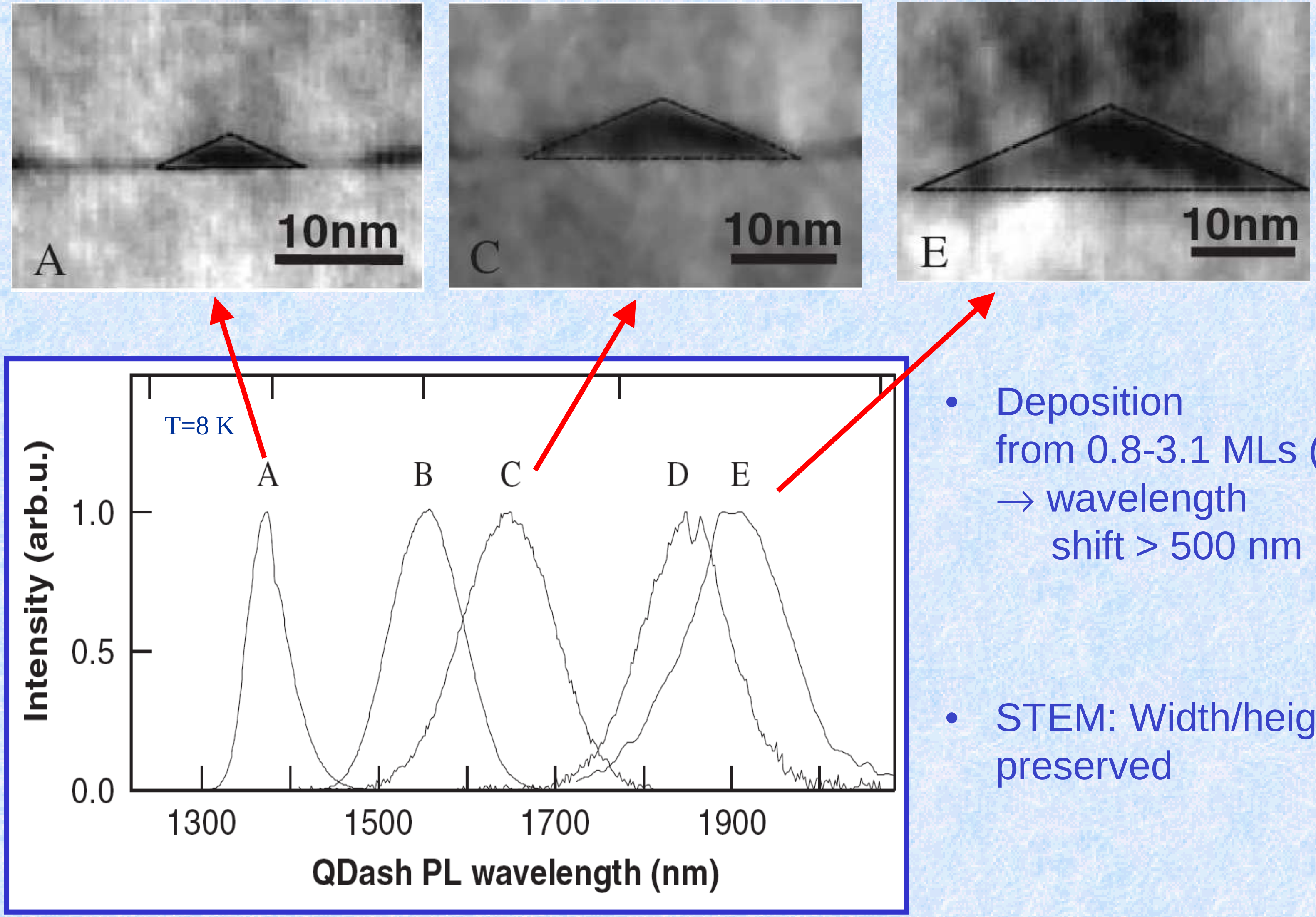

- Deposition from 0.8-3.1 MLs (A-E) $\rightarrow$ wavelength shift > 500 nm
- STEM: Width/height ratio preserved

T. Kümmell et al., Physica E 32, 108 (2006)

Variability of QDash Structures on InP

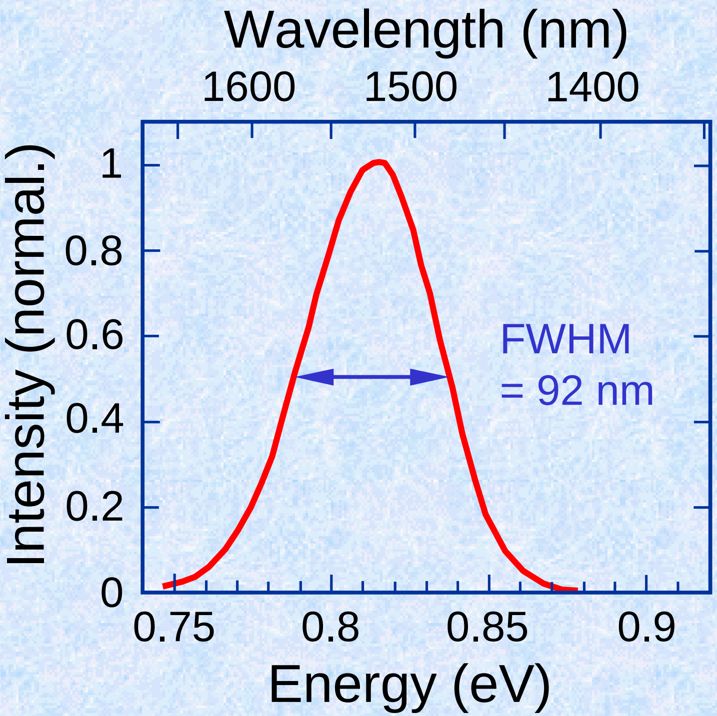

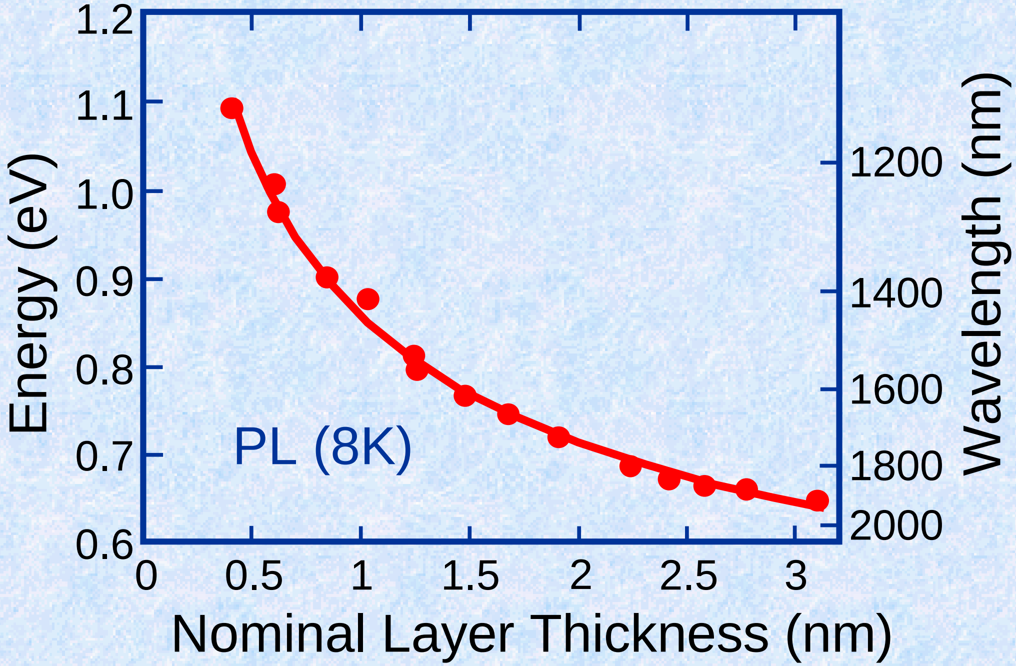

- Nearly symmetric broadband PL at 10 K
- Control of emission wavelength by QDash layer
- Extremely wide wavelength range: 1.2 – 2 µm (at RT)
- By multiple QDash layers ultra-broadband amplification possible

A. Somers, IPRM, Glasgow (2004)

Ultra-Broad Gain Spectrum

Design A 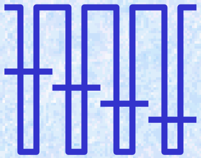 Design C 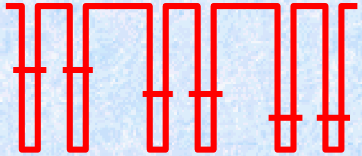

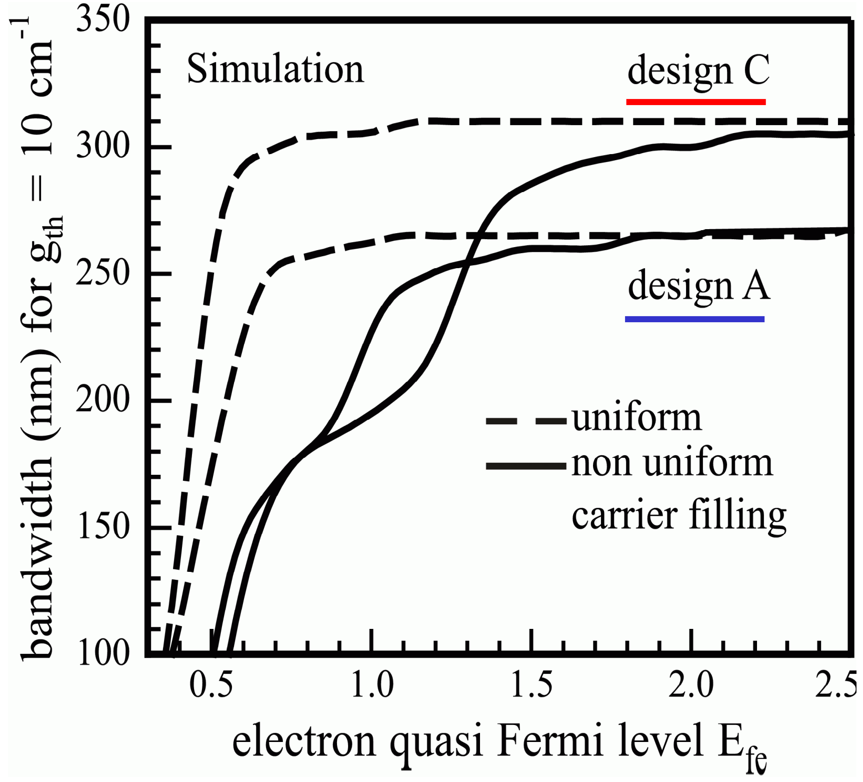

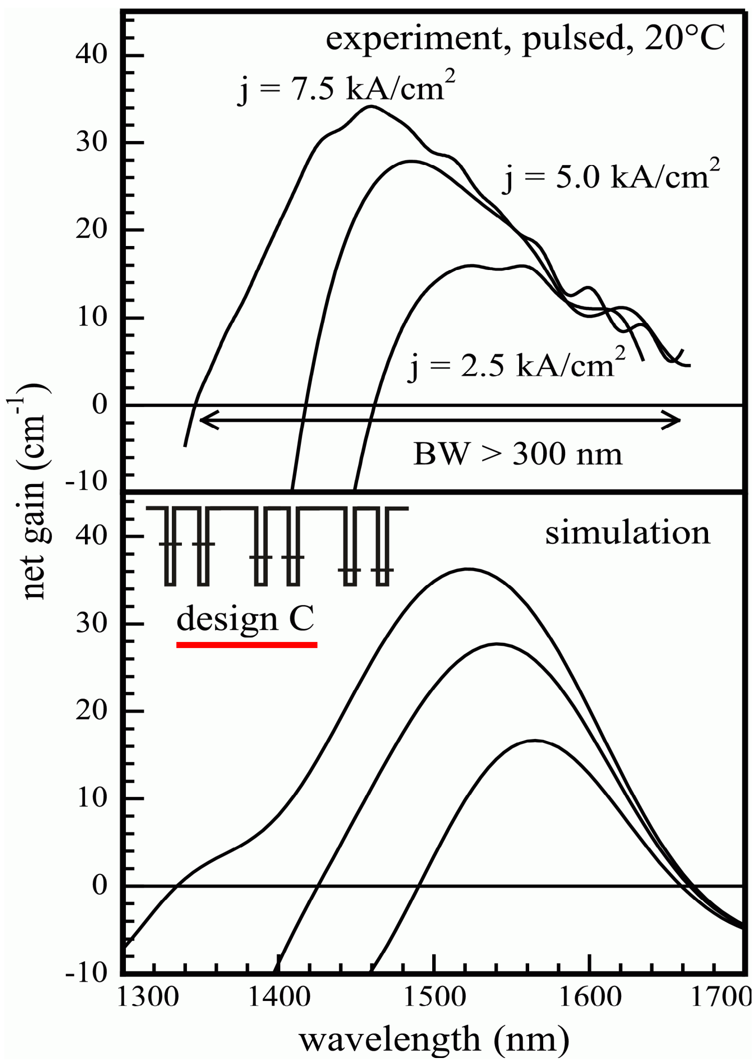

A. Somers et al., APL 89, 061107 (2006)

Static DFB Laser Data

RWG laser with HR coated backside mirror

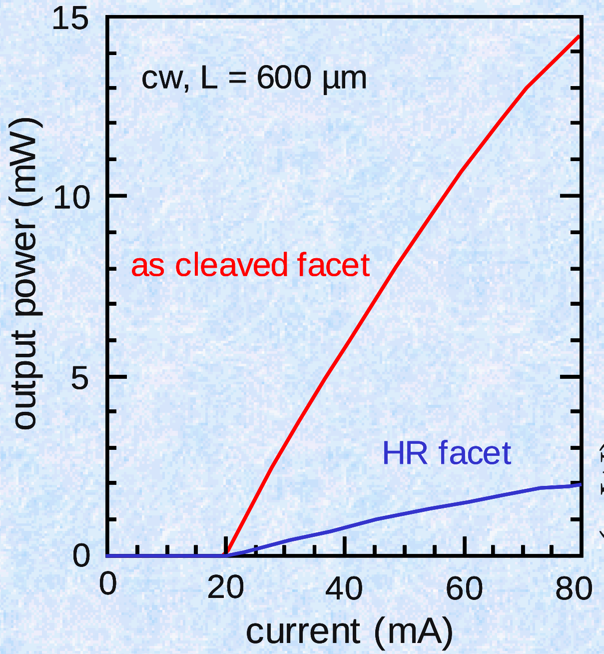

DFB laser with Cr gratings

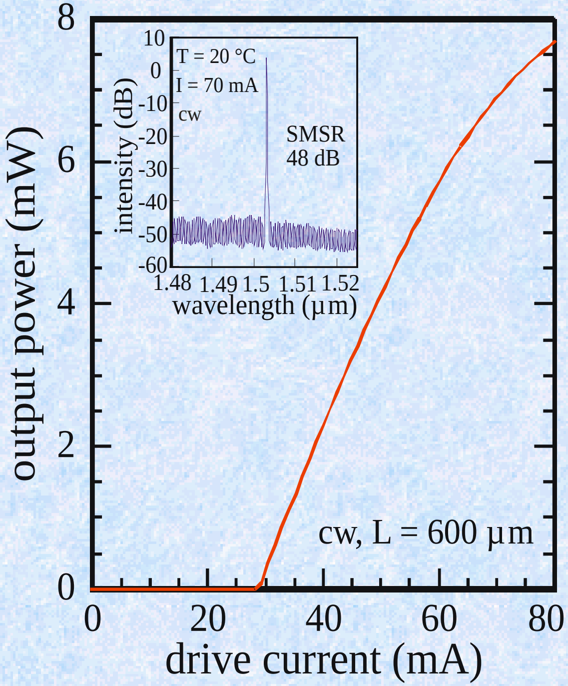

Single wafer

wavelength tuning

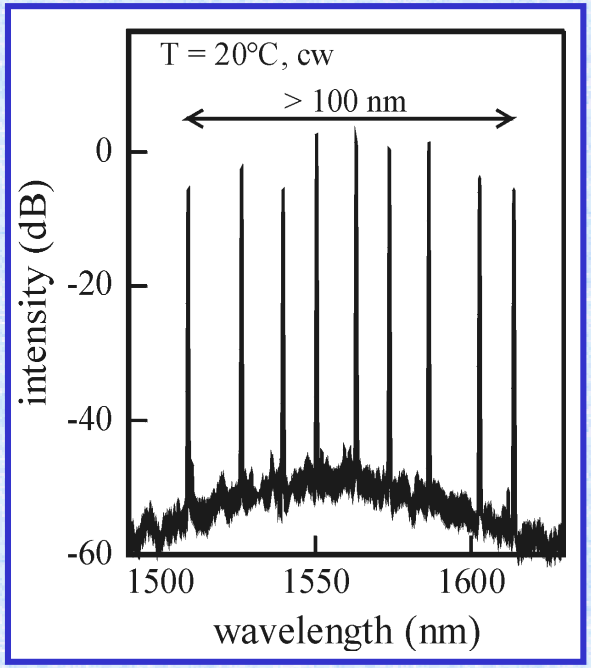

- Introduction and Some Basic Theory
  - density of states, gain function
  - dependence on dimensions
- Fabrication Technology
  - molecular beam epitaxy and Stranski-Krastanov growth mode
  - influence on geometry parameters
- Optical properties of real dots
  - single dot emission, higher order transitions
  - inhomogeneous linewidth, wetting layer
- Application examples of QD lasers
  - high power lasers (980 / 920 nm)
  - ultra-broad band lasers (1.55 µm)
  - ultra-fast broadband SOAs (1.55 µm)

Spectral gain of QD-SOAs

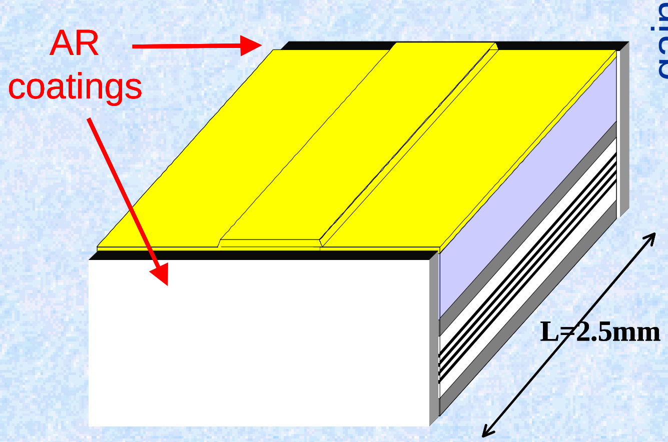

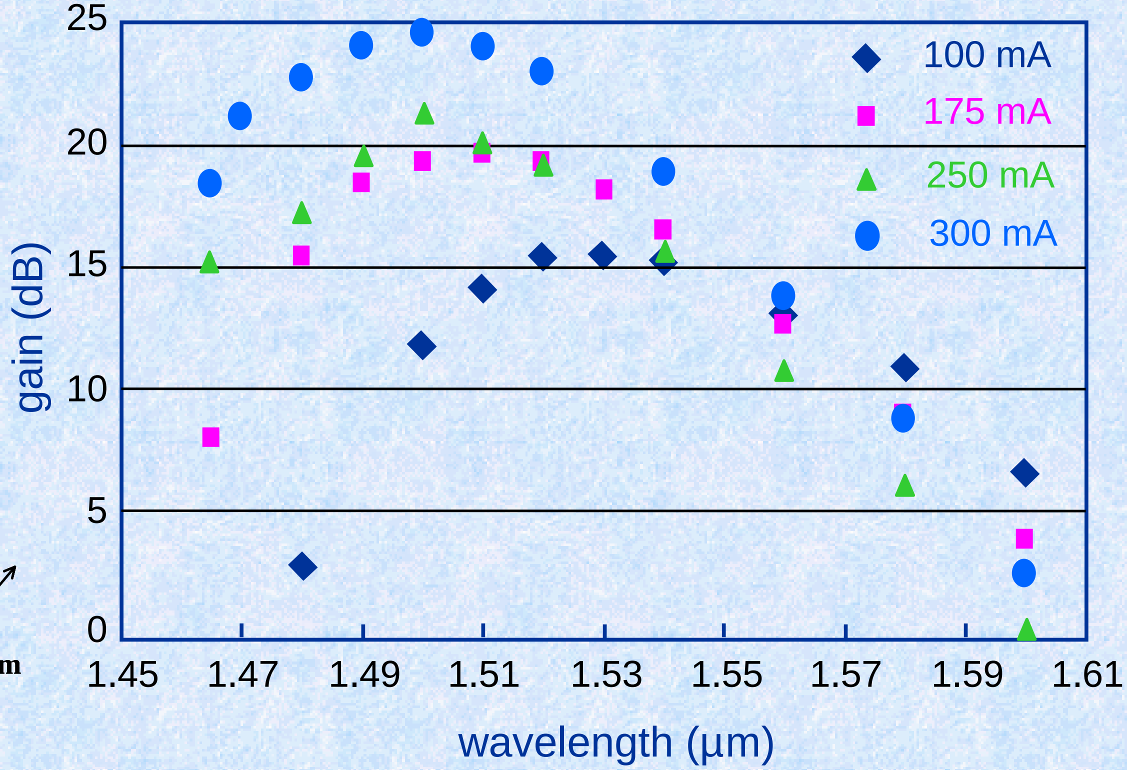

- SOA = RWG laser with anti-reflection coatings
- Large bandwidth (> 200 nm, measurments limited by tunable laser)
- High amplification (25 dB for 2.5 mm long device)
- High saturation power of 18 dBm (= 63 mW)

BER-Measurements for XG-Modulation

Technion

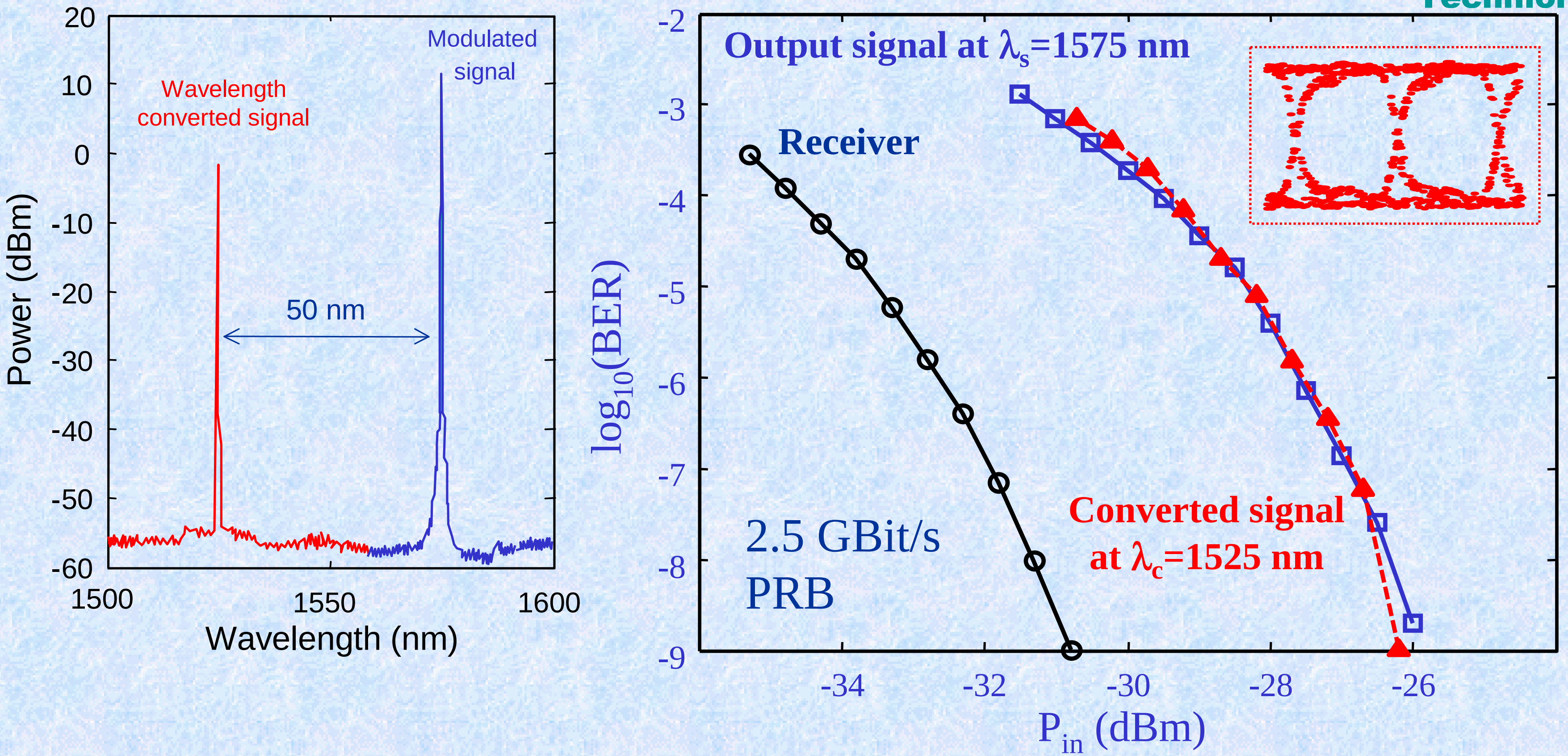

- About 5 dB penalty due to additional noise of amplifier and set-up
- 50 nm wavelength conversion with 2.5 Gbit/s (open eye diagram)
- BER identical between modulated and converted signal

A. Bilenca et al., PTL 15, 563 (2003)

Multi-wavelength amplification with QD-SOA

Technion

Amplification of eight 10 Gbit/s channels with no cross talk

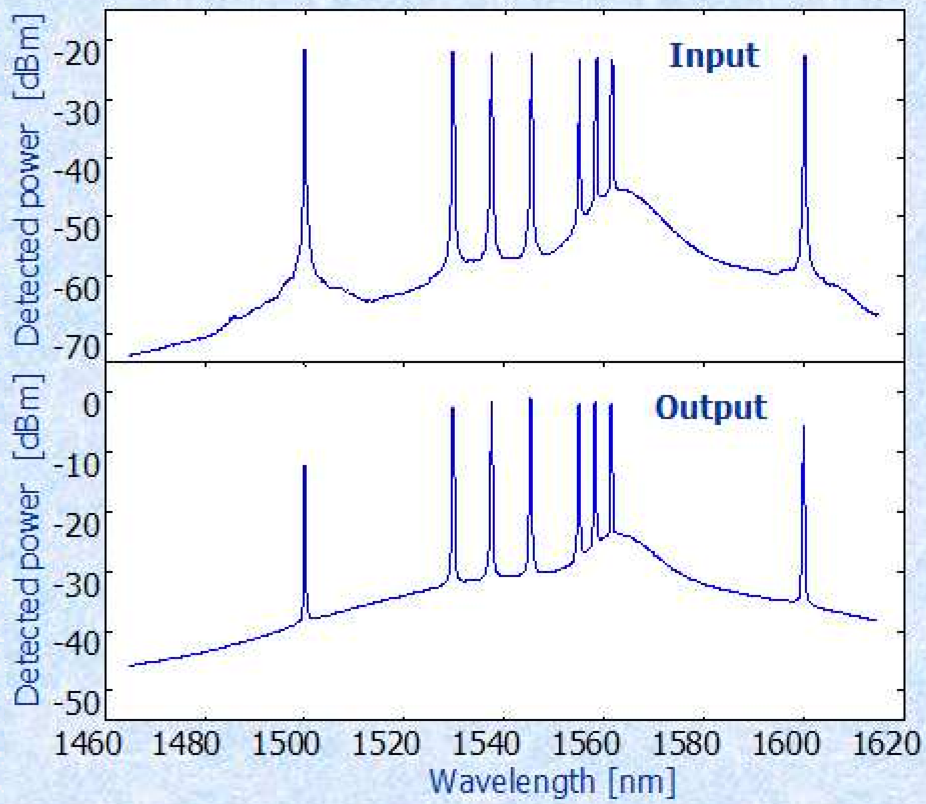

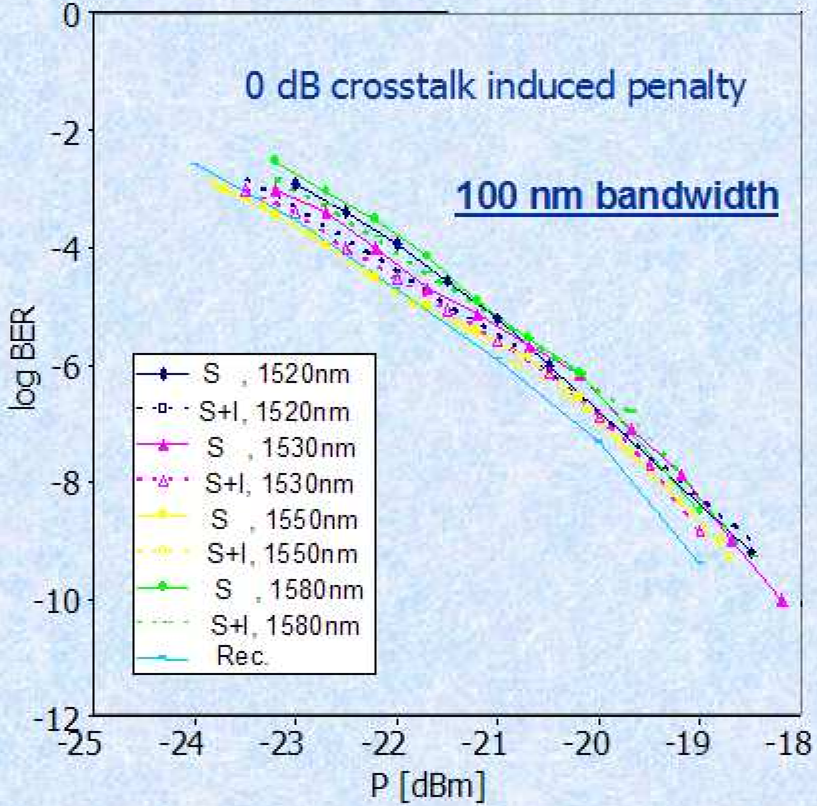

- Amplification of 8 channels over 100 nm at 10 Gbit/s
- P_{in} -21 dBm / channel - 0 dB crosstalk-induced penalty

R. Alizon et al., EL 40, 760 (2004)

HF Properties (40 Gbit/s)

Technion

ER 6.3
Q 4.15

ER 6.2
Q 4.5

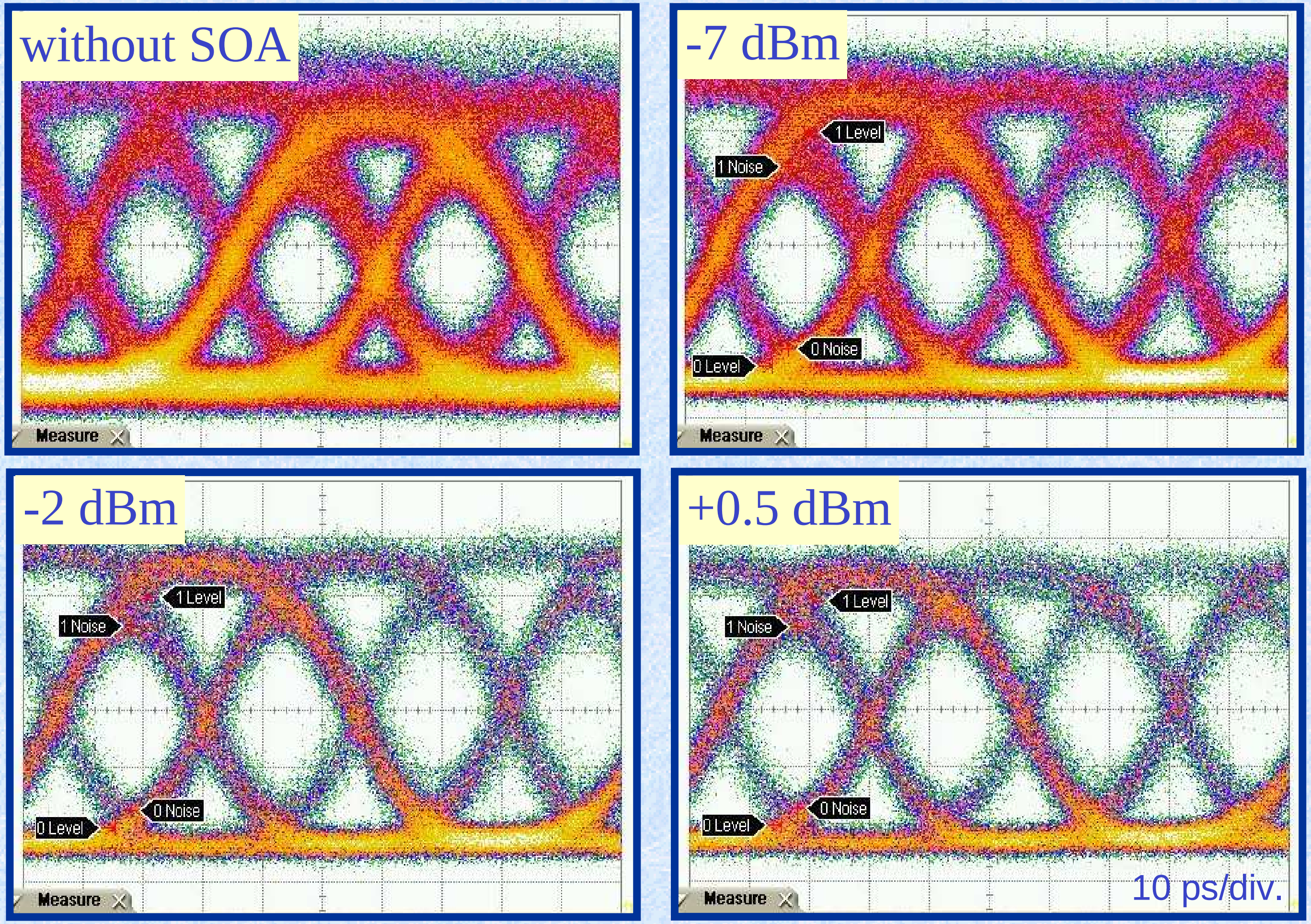

ER 6.1
Q 5.0

ER 5.9
Q 5.3

- 40 GBit/s PRB input signal: no patterning effect
- Improved signal for operation in saturation condition

J.P. Reithmaier et al., JPD 38, 2088 (2005)

Calculated RIN Spectra

Technion

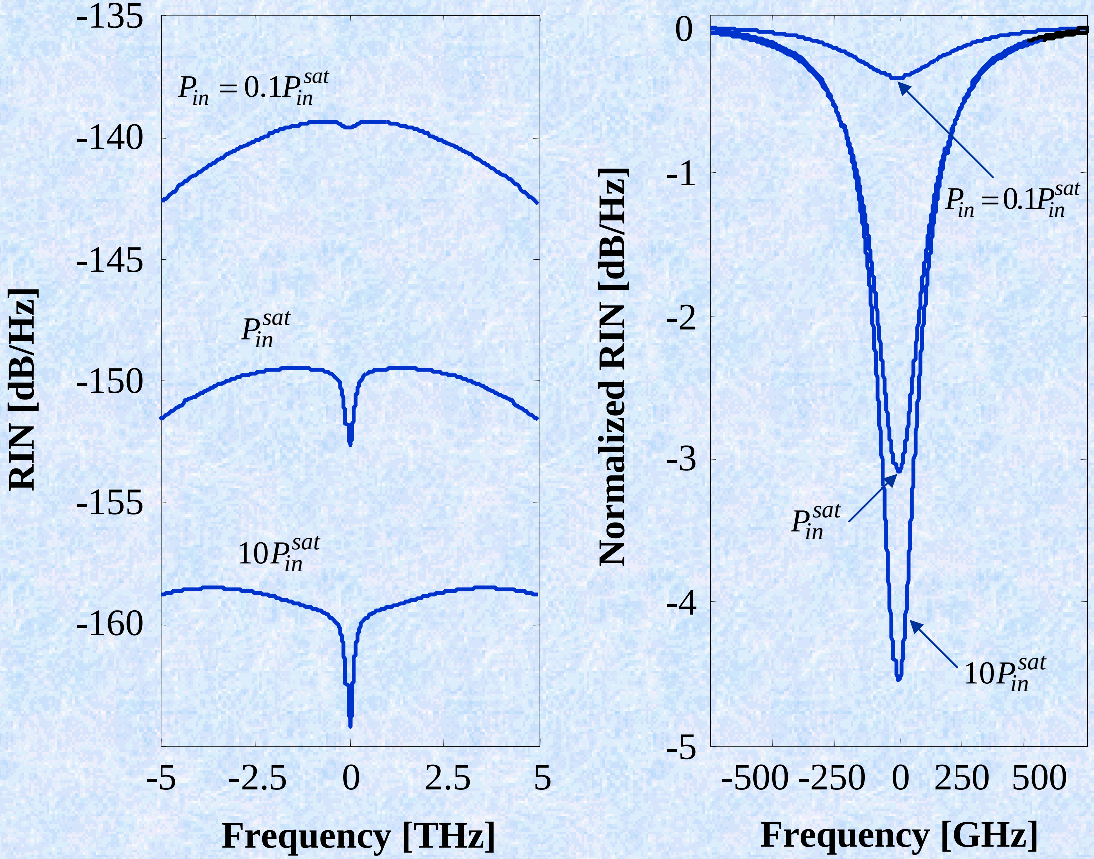

- Reduction in RIN signal due to band filling
- Broad band intensity noise suppression over hundreds of GHz !

D. Hadass, JSTQE 11, 1015 (2005)

Pump-Probe Measurements

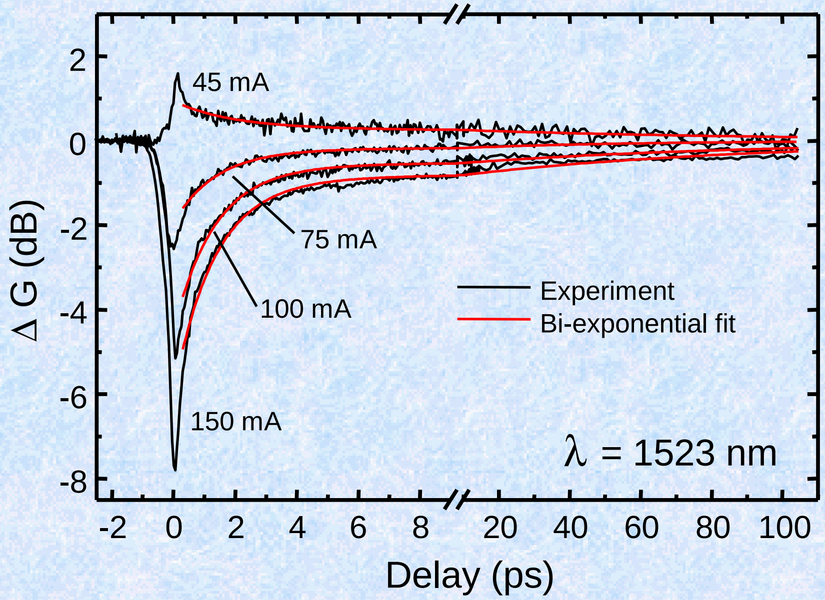

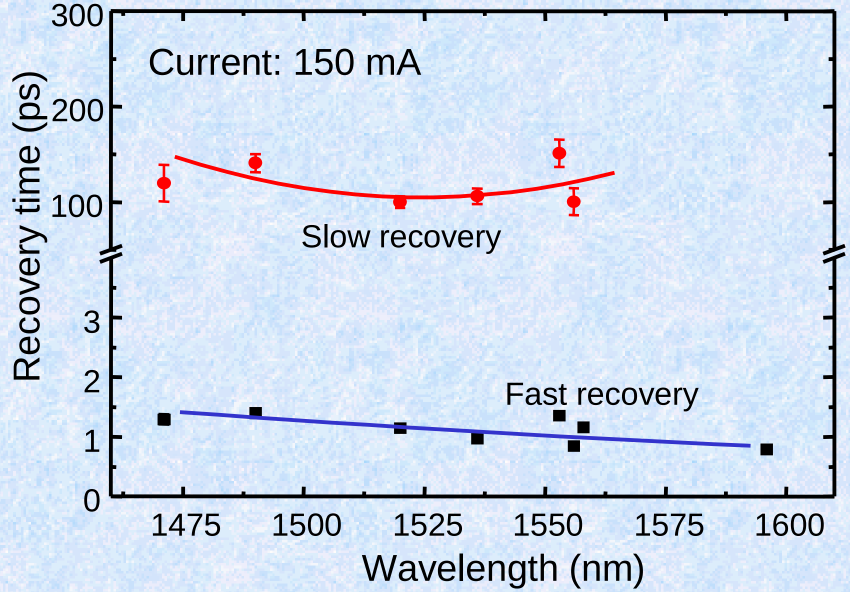

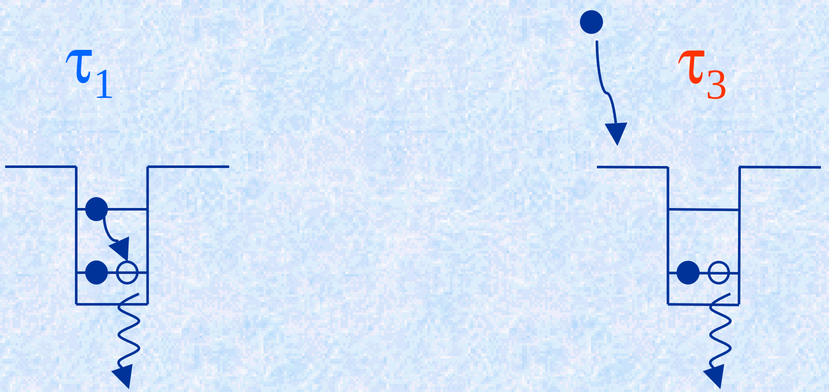

τ_1 = 1-2 ps (local carrier storage)
τ_3 > 100 ps (transport time)

M. Van der Poel et al., APL 89 (8), 081102 (2006)

Summary

- **Theoretical Background of Low Dimensional Systems**
  - Strong influence of dimensionality on gain properties
  - Additional geometry parameters can be used for spectral gain engineering and tailoring of new material properties
- **Fabrication Technology of Dot-Like Structures**
  - Self-assembly techniques driven by material strain
  - Geometry parameters (density, size, size distribution) can be controlled by growth parameters
- **High power QD lasers**
  - BA laser: 6.3 W (980 nm), 3 W (920 nm) output power, η_w = 55 %
  - Tapered laser: 3 W cw single lobe output power, η_w = 39%
  - Internal temperature compensation by dot tailoring (BA laser: $d\lambda/dT$ = 0.11 nm/K, T laser: $d\lambda/dT$ = 0.07 nm/K)
- **1.55 µm QD Lasers and SOAs**
  - ultra-broad band gain material (> 300 nm) for telecom laser appl.
  - 10 GBit/s multi-wavelength amplification
  - 40 GBit/s pattern free signal amplification and recovery

Acknowledgements

University of Würzburg

Thales R & T

Alcatel – Thales III-V Lab

Ferdinand Braun Institut
für Höchstfrequenztechnik

Technion

DTU•COM

Universidad Politécnica
de Madrid

Politecnico di Torino

European IST-Projects

ULTRABRIGHT

BRIGHT•EU

WWW•BRIGHTER•EU

BigBand

QPhoton